

RESEARCH ARTICLE

M proteins of group A *Streptococcus* bind hyaluronic acid via arginine–arginine/serine–arginine motifs

Tahnee B.-D. McEwan¹  | David M. P. De Oliveira^{1,2}  | Emily K. Stares¹ |
Lauren E. Hartley-Tassell³  | Christopher J. Day³  | Emma-Jayne Proctor¹  |
Victor Nizet⁴  | Mark J. Walker²  | Michael P. Jennings³  | Ronald Sluyter¹  |
Martina L. Sanderson-Smith¹ 

¹Molecular Horizons Research Institute and School of Chemistry and Molecular Bioscience, University of Wollongong, Wollongong, New South Wales, Australia

²Institute for Molecular Biosciences, The Centre for Superbug Solutions, The University of Queensland, St Lucia, Queensland, Australia

³Institute for Biomedicine and Glycomics, Griffith University, Gold Coast, Queensland, Australia

⁴Department of Pediatrics, University of California, San Diego, California, USA

Correspondence

Martina L. Sanderson-Smith, School of Chemistry and Molecular Bioscience, Faculty of Science, Medicine and Health, University of Wollongong, Wollongong, NSW 2522, Australia.

Email: martina@uow.edu.au

Present address

Tahnee B.-D. McEwan, Sutton Arthritis Research Laboratory and the Australian Arthritis and Autoimmune Biobank Collaborative (A3BC), Sydney Musculoskeletal Health, Kolling Institute, The University of Sydney and the Northern Sydney Local Health District, Sydney, New South Wales, Australia

David M. P. De Oliveira, Institute for Molecular Biosciences, The Centre for Superbug Solutions, The University of Queensland, St Lucia, Queensland, Australia

Emily K. Stares, Teva Pharmaceuticals, Macquarie Park, New South Wales, Australia

Funding information

DHAC | National Health and Medical Research Council (NHMRC), Grant/Award Number: APP1143266 and 1138466

Abstract

Tissue injury, including extracellular matrix (ECM) degradation, is a hallmark of group A *Streptococcus* (GAS) skin infection and is partially mediated by M proteins which possess lectin-like properties. Hyaluronic acid is a glycosaminoglycan enriched in the cutaneous ECM, yet an interaction with M proteins has yet to be explored. This study revealed that hyaluronic acid binding was conserved across phylogenetically diverse M proteins, mediated by RR/SR motifs predominantly localized in the C repeat region. Keratinocyte wound healing was decreased through the recruitment of hyaluronic acid by M proteins in an M type-specific manner.

Abbreviations: ECM, extracellular matrix; FBS, foetal bovine serum; GAGs, glycosaminoglycans; GAS, group A *Streptococcus*; GST, glutathione-S-transferase; NTA, nitrilotriacetic acid; PAGE, polyacrylamide gel electrophoresis; PBS, phosphate-buffered saline; RR/SR, arginine–arginine/serine–arginine; SDS, sodium dodecyl sulfate; SPR, surface plasmon resonance.

Tahnee B.-D. McEwan, David M. P. De Oliveira, and Emily K. Stares are no longer at the institutions where the work was performed.

This is an open access article under the terms of the [Creative Commons Attribution](https://creativecommons.org/licenses/by/4.0/) License, which permits use, distribution and reproduction in any medium, provided the original work is properly cited.

© 2024 The Author(s). *The FASEB Journal* published by Wiley Periodicals LLC on behalf of Federation of American Societies for Experimental Biology.

GAS strains 5448 (M1 serotype) and ALAB49 (M53 serotype) also bound hyaluronic acid via M proteins, but hyaluronic acid could increase bacterial adherence independently of M proteins. The identification of host–pathogen mechanisms that affect ECM composition and cell repair responses may facilitate the development of nonantibiotic therapeutics that arrest GAS disease progression in the skin.

KEYWORDS

adherence, binding motif, glycosaminoglycan, M protein, mutagenesis, *Streptococcus pyogenes*, surface plasmon resonance, wound healing

1 | INTRODUCTION

Streptococcus pyogenes (group A *Streptococcus*; GAS) is a human-specific bacterial pathogen, recognized globally as one of the leading causes of infectious disease mortality.¹ As a colonizer of both epithelial and mucosal tissue, GAS is responsible for causing a broad spectrum of pathologies, ranging from self-limiting infections to systemic diseases and post-streptococcal immunological sequelae such as rheumatic heart disease.² The global resurgence in invasive GAS disease³ has heightened an interest in understanding the pathogenic mechanisms that facilitate the initial stages of infection. An essential prerequisite for establishing GAS infection is effective adherence to host cells, enabling colonization.⁴ Compromised host physiological barriers facilitate both the systemic dissemination of GAS and persistent infection. Fundamentally, the degradation of protective outer networks such as the extracellular matrix (ECM) occurs in the early stages of invasive GAS pathogenesis and is a hallmark of tissue injury.^{5–7} ECM degradation can occur directly through the secretion of GAS virulence factors, the recruitment of host proteases, or via host-mediated processes presenting a means for opportunistic infection.^{2,8,9} These processes can lead to delays in wound healing and tissue repair, contributing to the persistence of GAS infections.^{10,11} Current treatment failure rates reinforce the need to identify new host targets for therapeutic intervention.^{12,13}

The M protein of GAS is partially responsible for ECM degradation during infection through plasmin(ogen) acquisition, inadvertently delaying wound healing.^{2,14} Moreover, the M protein is recognized as a major adhesin of GAS with emerging evidence of lectin-like properties.^{15,16} Glycosaminoglycans (GAGs) are a key component of the ECM, and while it has been shown that M proteins can interact with a variety of GAG subclasses to facilitate adherence,¹⁷ interactions with host hyaluronic acid have not been reported. Hyaluronic acid is the largest negatively charged mucopolysaccharide among GAGs (10¹–10⁴ kDa),¹⁸ with each disaccharide unit

consisting of a uronic sugar (D-glucuronic acid) covalently linked to an amino sugar (N-acetylglucosamine)¹⁹ (Figure 1A). Endogenous hyaluronic acid is enriched in the cutaneous ECM and is found in high concentrations surrounding keratinocytes in the skin, where it plays integral roles in immune surveillance and wound healing.²⁰

Recent evidence suggests that host hyaluronic acid acts as a modulator of GAS virulence, with distinct roles dependent on chain length. High molecular weight hyaluronic acid has been shown to entrap GAS at the surface of immune cells reducing internalization, yet an increase in the conversion of high to low molecular weight hyaluronic acid in vivo, a process analogous to ECM breakdown, was shown to enhance GAS phagocytosis by infiltrating macrophages.²¹ Whether this pro-inflammatory hyaluronic acid has a role in modulating GAS adherence or wound healing during infection, and which GAS proteins mediate these interactions, have yet to be addressed. Therefore, the aim of this study was to provide a novel characterization of M proteins functioning as receptors for host hyaluronic acid and to investigate the physiological relevance of this interaction. Here, we demonstrate that M proteins can bind exogenous hyaluronic acid via conserved RR/SR motifs localized to the C repeat region. This interaction was shown to decrease wound healing in an M type-specific manner, while hyaluronic acid could increase bacterial adherence independently of M proteins.

2 | MATERIALS AND METHODS

2.1 | Glycosaminoglycans

Select-HA™ hyaluronan (a mixture of 25–75 kDa chains, Cat# S0451), hyaluronic acid sodium salt (a mixture of 1000–4000 kDa chains, Cat# H5388), and fluorescein-conjugated hyaluronic acid (a mixture of 640–1000 kDa chains, Cat# F1177) were from Sigma-Aldrich (St Louis, MO, USA). Epimer configuration was not disclosed by suppliers. Hyaluronic acid sodium salt was utilized for

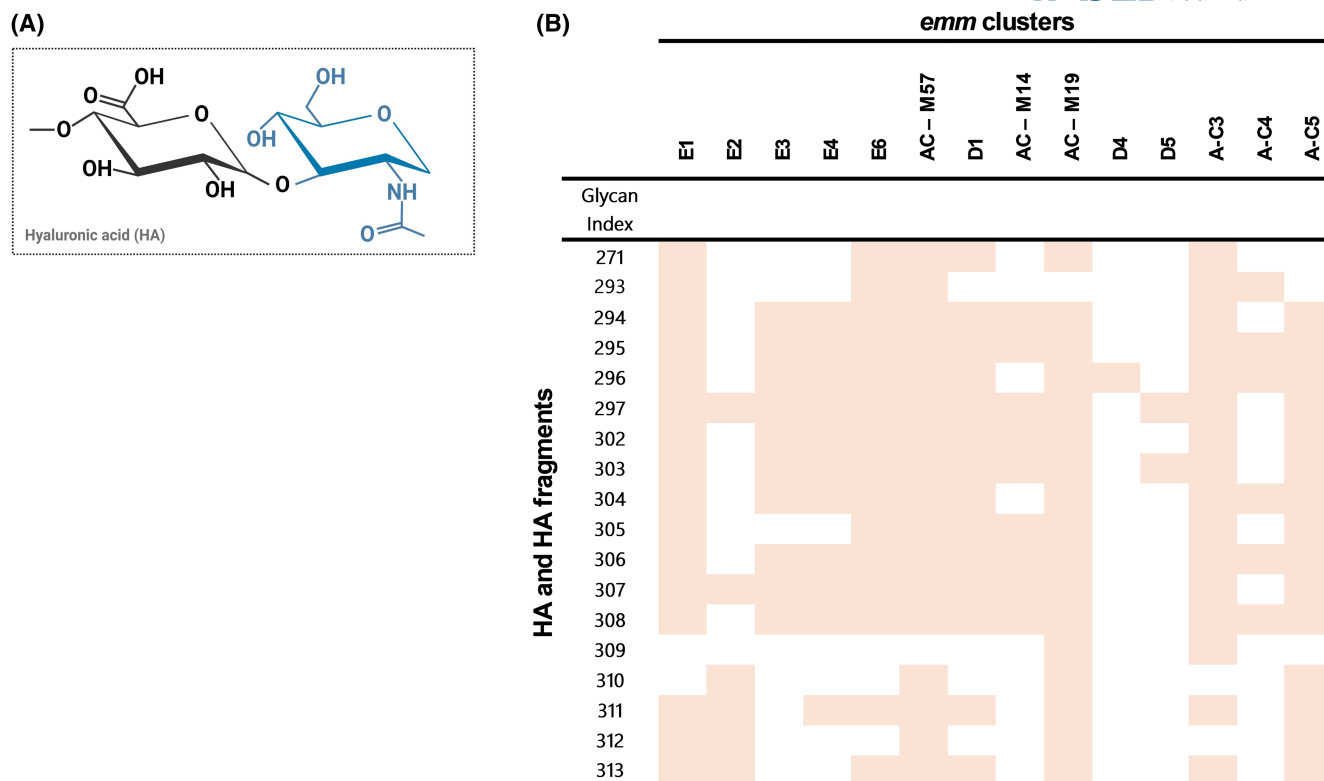


FIGURE 1 Hyaluronic acid binding is a conserved function across phylogenetically diverse M proteins. (A) Primary configuration of hyaluronic acid (HA) is represented consisting of D-glucuronic acid (black) and N-acetylglucosamine (blue). Heterogeneity arises from chain length and/or epimerization. Created with BioRender. (B) Binding profile of HA and HA fragments with phylogenetically clustered M protein using a glycan microarray. Orange blocks, indicative of glycan binding, are presented only if all M protein representatives within a cluster group (M1, M2, M3, M9, M11, M12, M14, M19, M53, M54, M57, M58, M60, M65, M70, M90, M97, M98, M102, and M106) were able to bind the respective HA structure from three independent experiments.

experiments involving fluorescein-conjugated hyaluronic acid and bacterial aggregation assays, while Select-HA™ hyaluronan was utilized for surface plasmon resonance (SPR), wound healing and adherence assays.

2.2 | Expression vectors

The *emm* genes that were cloned into expression vectors pGEX-2T or pET-41 contained glutathione-S-transferase (GST) tags as previously described.²² M protein fragment constructs in a pET-28b(+) vector were designed as previously described,^{23–25} and synthesized by GenScript Biotech. A 6×His-tag (LEHHHHHH) was integrated into all sequences at the C-terminus.

2.3 | Recombinant protein expression and purification

Top10 and BL21(DE3) *Escherichia coli* containing expression vectors were cultured at 37°C with shaking in Luria-Bertani broth supplemented with 50 µg/mL

kanamycin sulfate or 100 µg/mL ampicillin. Recombinant protein expression and purification by GST affinity chromatography was conducted as previously described.²⁶ Thrombin-cleaved M proteins or clarified *E. coli* lysates containing recombinant M protein fragments were further purified using Ni²⁺–nitrilotriacetic acid (NTA) affinity chromatography. Unbound proteins were removed with washing buffer (50 mM NaH₂PO₄, 300 mM NaCl, 250 mM imidazole-hydrochloride, pH 8.1) and proteins were eluted using native elution buffer [50 mM NaH₂PO₄, 300 mM NaCl, 20 mM imidazole-hydrochloride, 20% (v/v) glycerol, pH 8.5]. M protein fragments were further purified using anionic Mono Q™ 5/50 GL or cationic HiTrap™ CM Sepharose FF exchange columns assembled in a Next Generation Chromatography system unit (Bio-Rad, Hercules, CA, USA). M protein fragments were washed (20 mM Tris–HCl, 1 mM EDTA tetrasodium salt, 0.02% (w/v) NaN₃; pH 8.5 or pH 6.5) and collected using a 0%–25% (v/v) gradient elution buffer [0–500 mM final; 20 mM Tris–HCl, 1 mM EDTA tetrasodium salt, 2 M NaCl, 0.02% (w/v) NaN₃, pH 8.5]. All recombinant M proteins and M protein fragments were concentrated using polyvinylpyrrolidone and dialysed in phosphate-buffered saline (PBS).

2.4 | GAS strains and culture conditions

5448 (*emm1*) is a hypervirulent M1T1 clone originally isolated from invasive soft tissue infection.^{27,28} ALAB49 (*emm53*) was originally isolated from noninvasive impetigo infection.^{29,30} Isogenic M protein-deletion mutants 5448 Δ *emm1* and ALAB49 Δ *pam* and their respective reverse complementation strains 5448 Δ *emm1* RC and ALAB49 Δ *pam* RC have been described elsewhere.^{30,31} All GAS strains were routinely cultured statically at 37°C in 3% (w/v) Todd-Hewitt broth (BD Biosciences, Franklin Lakes, NJ, USA) supplemented with 1% (w/v) yeast (in absence or presence of 5 µg/mL erythromycin, 200 µg/mL kanamycin sulfate or 100 µg/mL spectinomycin) before harvesting at mid-logarithmic phase [OD_{600} 0.3 for all ALAB49-derived strains or OD_{600} 0.4 for all 5448-derived strains, consistent with previous reports^{30,32}].

2.5 | Preparation of GAS cell wall extracts

GAS cell wall extracts were prepared as described³³ with minor modifications. Mid-logarithmic GAS were harvested by centrifugation (7500g, 20 min, 4°C) and washed twice with ice-cold sterile TE buffer (50mM Tris, 1mM EDTA, pH8.0) supplemented with 1mM phenylmethylsulfonyl fluoride (7500g, 20 min, 4°C). Cell pellets were resuspended in mutanolysin mix [10mg/mL lysozyme and 62.5U/mL mutanolysin in 20% (w/v) sucrose/TE buffer] and incubated at 37°C with orbital shaking at 180rpm for 2.5h. Supernatants containing the mutanolysin cell wall extract were collected (16000g, 5 min).

2.6 | Isolation of GAS supernatants

Mid-logarithmic phase GAS were centrifuged (7500g, 20 min, 4°C) and supernatants were collected and syringe-filtered (0.22 µm filter). Soluble proteins were concentrated using 10% (w/v) ice-cold trichloroacetic acid at a ratio of 1:1 for 30 min on ice. Extracts were centrifuged (16000g, 20 min, 4°C) and washed twice with ice-cold acetone (16000g, 20 min). Pellets were air dried at room temperature for 30 min.

2.7 | GAS growth kinetic curves

Overnight starter cultures of GAS were diluted 1:10 into a 96-well plate (Frickenhausen, Germany) containing culture media (with or without selective antibiotics) in absence or

presence of 1 µM hyaluronic acid and incubated at 37°C for 16 h in a CLARIOstar plate reader (BMG Labtech, Ortenberg, Germany). Measurements were taken every 10 min (orbital averaging after 30-s shake) at 600 nm.

2.8 | GAS autoaggregation assay

Vortexed overnight starter cultures of GAS were incubated in absence or presence of hyaluronic acid (500 µg/mL) at room temperature to monitor sedimentation. Measurements of the upper phase were recorded every hour for 7 h using a CLARIOstar plate reader. Bacterial aggregation was calculated as described previously³⁴ using the following equation: Aggregation (%) = $1 - (OD_{7h} / OD_{0h})$.

2.9 | Mammalian cell culture

HaCaT human keratinocytes (CLS Cat# 300493/p800_HaCaT, RRID:CVCL_0038) were authenticated by short tandem repeat profiling and routinely tested negative for mycobacterial contamination.³⁵ Cells were maintained in Dulbecco's modified Eagle's medium: Nutrient Mixture F-12 (DMEM/F12; Thermo Fisher Scientific, Waltham, MA, USA) containing heat-inactivated 10% (v/v) foetal bovine serum (FBS; Bovogen Biologicals, Melbourne, Australia), 2mM GlutaMAX, 100 U/mL penicillin and 100 µg/mL streptomycin at 37°C/5% CO₂ and passaged using 0.05% trypsin-EDTA.

2.10 | Polyacrylamide gel electrophoresis (PAGE) and immunoblotting

Recombinant M proteins (200 ng–2 µg) were subjected to a reducing 12% (v/v) sodium dodecyl sulfate (SDS)-PAGE and visualized using Coomassie R-250 Rapid staining.³⁶ Recombinant M protein fragments (200 ng–2 µg) were subjected to a reducing 10% (v/v) Tris-tricine PAGE and visualized using Colloidal Blue staining.³⁷ Proteins from bacterial cell lysates and supernatants (15–20 µg) were loaded and separated via Tris-tricine PAGE under reducing conditions using pre-cast Mini-Protean TGX Stain-Free gels (4%–20%; Bio-Rad). Samples were transferred onto a methanol-activated polyvinylidene difluoride membrane and blocked overnight at 4°C using 5% (w/v) skim milk powder in PBS supplemented with 0.1% (v/v) Tween® 20. Membranes were incubated with primary rabbit anti-M protein sera (1:30000; in-house²⁶) for 1.5 h at room temperature. Membranes were washed thrice and re-probed using horseradish peroxidase-conjugated

goat anti-rabbit IgG (1:3000, AB_2533967, Cat# 65-6120; Thermo Fisher Scientific) for 1 h at room temperature prior to chemiluminescence detection.³⁸ For GAS supernatant expression analysis, immunoblots were first probed using rabbit anti-M protein sera (1:30000) and prepared for re-probing with rabbit polyclonal anti-SpeB sera (1:1000; Toxin Technology Inc., Sarasota, FL, USA) as described.³⁹ Mature and zymogen SpeB protein were included as positive controls (Toxin Technologies Inc.) while bovine serum albumin was included as a negative control. To assess purity of protein samples from gels or to quantify protein expression on immunoblots, densitometry was performed using Quantity One 1-D Analysis Software (version 4.6.7; Bio-Rad).

2.11 | Glycan microarray

Recombinant M protein–hyaluronic acid interactions were initially screened using a glycan microarray as previously described.¹⁵ Briefly, recombinant M proteins (0.5–1 µg) were complexed with mouse anti-histidine IgG, rabbit anti-mouse Alexafluor488 IgG conjugate and goat anti-rabbit Alexafluor488 IgG conjugate at a ratio of 4:2:1 and secured onto pre-blocked glycan microarray slides. Fluorescence was measured using a ProScanArray Microarray 4-Laser Scanner (Perkin Elmer, Waltham, MA, USA).

2.12 | Surface plasmon resonance

M protein–hyaluronic acid-binding interactions were detected in real time using Biacore T200 Control Software (version 3.2; Cytiva, Marlborough, MA, USA) using single-cycle kinetics at 25°C. All flow channels of a Series S NTA Sensor Chip (Cytiva, Marlborough, MA, USA) were activated using 0.5 mM NiCl₂ in running buffer [10 mM HEPES, 0.15 M NaCl, 50 µM EDTA, 0.05% (v/v) Tween® 20, pH 7.4] with excess ions removed using 3 mM EDTA. GAG binding has been shown to decrease in PBS solutions due to charged ions,⁴⁰ hence HEPES buffer was selected as it is zwitterionic, does not bind Ni²⁺, and has improved reproducibility.^{41,42} Purified His-tagged M proteins (200 nM) were immobilized (~350 response units) to designated flow channels^{2, 3, 4} at 10 µL/min. For each cycle, flow channel 1 was absent of bound protein and served as a blank control for internal subtraction. Reference subtraction within each designated flow cell immobilized with M protein was also included to account for bulk refractive index differences between system flow buffer and analyte buffer. Hyaluronic acid (0–200 nM) was flowed across all channels as a series of

five injections at 10 µL/min with a 180-s association time and a 30-s dissociation time. For each run, streptokinase (in-house) was included as a universal negative control as it did not bind any of the M proteins tested. For each cycle, human serum albumin (Cat# A3782; Sigma-Aldrich), fibrinogen (Cat# F48831; Sigma-Aldrich), plasminogen (Cat# HCPG-0130; Prolytix, Essex Junction, VT) and C4b-binding protein (Cat# 600672; Agilent technologies, Santa Clara, CA, USA) were included as positive controls for specific M proteins.²² Interactions were evaluated using steady-state affinity analysis on Biacore T200 evaluation software (version 3.2; Cytiva), which followed a 1:1 Langmuir binding model.⁴³

2.13 | Fluorescence plate-based binding assay

Recombinant wild-type and mutant M53 protein and bovine serum albumin (20 µg/mL in 0.1 M NaHCO₃, pH 9.6) were coated in a 96-well black-walled µClear® bottom medium binding plate (Greiner Bio-One, Frickenhausen, Germany) at 4°C overnight and washed twice with PBS. Proteins were incubated in the absence or presence of unlabelled hyaluronic acid in 30-fold excess (3 mg/mL) for 2 h at room temperature with gentle agitation. Fluorescence in the presence of excess unlabelled hyaluronic acid was used as a proxy for nonspecific binding; nonspecific interactions were subtracted from total M protein–hyaluronic acid interactions to determine specific interactions. Plates were washed thrice and incubated with fluorescein-labeled hyaluronic acid (100 µg/mL) for 2 h at room temperature with gentle agitation. Plates were washed five times before fluorescence measurements were recorded using a CLARIOstar (4 × 4 matrix well scanning; excitation, 483/14 nm; emission, 530/30 nm).

2.14 | In vitro scratch wound assay

An in vitro scratch wound model was established as previously described.³⁵ Briefly, HaCaT keratinocyte monolayers were uniformly scratched using a 96-pin WoundMaker (Essen Bioscience, Ann Arbor, MI) and incubated in absence (Nil, medium alone) or presence of 50 µg/mL M53 proteins or M1 proteins, and/or 10 µg/mL hyaluronic acid in DMEM/F12 containing 0.2% (v/v) FBS, 2 mM GlutaMAX, 100 U/mL penicillin and 100 µg/mL streptomycin. Images were captured and analyzed over time using phase-contrast microscopy with IncuCyte ZOOM live cell imaging software (Essen Bioscience). To determine the percent of relative wound

closure over 24 h (%), the area under the curve for each sample was calculated and normalized to the response of the nil control.

2.15 | Flow cytometry

Mid-logarithmic GAS strains (1×10^6 cells) were washed with PBS and pre-incubated in the absence or presence of unlabelled hyaluronic acid in 5-fold excess (1.25 mg/mL) on ice for 1 h. Fluorescence in the presence of excess unlabelled hyaluronic acid was used as a proxy for non-specific binding; nonspecific interactions were subtracted from total GAS–hyaluronic acid interactions to determine specific interactions. Cells were washed and incubated with 200 µg/mL fluorescein-labeled hyaluronic acid, and 10 µg/mL cell viability dye 7-Aminoactinomycin D for 1 h on ice protected from light. Labeled cells were washed and collected using a BD LSR Fortessa X-20 flow cytometer (BD Biosciences). Data were acquired using the following settings: Standard cell architecture and fluorescein (excitation, 488 nm; emission, 525/50 nm) and 7-Aminoactinomycin D (excitation, 561 nm; emission, 670/30 nm).

2.16 | Quantitative PCR

Mid-logarithmic GAS ($1\text{--}2 \times 10^7$) were resuspended in enzymatic lysis buffer [20 mg/mL lysozyme, 20 mM Tris–HCl, 2 mM EDTA disodium salt, 1.2% (v/v) Triton® X-100, pH 8.0] and incubated statically for 30 min at 37°C. RNA was isolated using an Aurum™ Total RNA Fatty And Fibrous Tissue Module DNA-Free RNA Isolation Kit (Bio-Rad) with DNase I treatment, as per the manufacturer's instructions. Residual genomic DNA was removed using a Turbo DNA-free™ Kit (Thermo Fisher Scientific) as per the manufacturer's instructions and cDNA was synthesized using a High-Capacity cDNA Reverse Transcription Kit (Thermo Fisher Scientific). Bacterial gene expression was assessed using a SYBR GreenER™ SuperMix Universal Kit (Thermo Fisher Scientific) according to the manufacturer's instructions. Primer sets *emmY1* and *emmY2* were utilized to quantify M protein gene expression in 5448 and ALAB49 respectively, with *recA* as the housekeeping gene as previously described.⁴⁴ Gene expression analyses and melt curves were conducted using a Quant Studio 5 real time PCR System (Thermo Fisher Scientific). Reactions were analyzed using QuantStudio Design and Analysis Software (version 1.5.1; Thermo Fisher Scientific). Relative fold gene expression was quantified using the ΔCt method^{45,46} where the genes of interest were

normalized to the GAS housekeeping gene. Serial dilutions of cDNA were used to determine the primer efficiencies of *emmY1* and *emmY2* primer sets.

2.17 | GAS adherence assay

A keratinocyte cell adherence assay by GAS was adapted from a previous study.¹⁵ Mid-logarithmic GAS (2.5×10^5 cells) were pre-incubated with 1 µM hyaluronic acid (or corresponding vehicle) statically for 30 min at room temperature. Cells were equilibrated in antibiotic-free DMEM/F12 supplemented with 10% (v/v) FBS and 2 mM GlutaMAX and added to HaCaT keratinocyte monolayers at a MOI of 5:1. Plates were centrifuged (300g, 5 min) and incubated for 1 h at 37°C. Nonadherent bacteria were removed by washing twice with sterile PBS. To assess total bacterial cell association (adherence and invasion), GAS-bound HaCaT keratinocytes were detached using 500 U/mL accutase with a 10 min incubation at 37°C followed by 0.025% (v/v) Triton® X-100 for cell lysis. Well selection for medium extraction was randomized to minimize count bias. A 10-fold serial dilution was performed, and spot plated for bacterial enumeration. To measure GAS invasion only, GAS-bound HaCaT keratinocytes were pre-treated with 100 µg/mL gentamicin sulfate as described previously.¹⁵ Bacterial counts (CFU) were normalized to the original inoculum. The level of GAS cell adherence was determined by subtracting the percentage (%) of internalized GAS from the percentage (%) of total associated GAS.

2.18 | Bioinformatic analyses

Annotated nucleotide sequences (*emm*) for M proteins were retrieved from the GenBank (National Center for Biotechnology Information) database for structural domain mapping using the following accession numbers: M1 [WP_011285743.1 or CP008776.1 (5448) and JX028599.1], M2 (JX028602.1), M3 (JX028602.1), M9 (KC978828.1 or JX028608.1), M12 (WP_002991230.1), M14 (JX028612.1), M19 (JX028616.1), M53 (P49054.1), M54 (JX028645.1), M57 (A44643), M60 (JX028651.1) and M65 (JX028651.1). Mature M protein sequences were trimmed to the last amino acid residue prior to D repeat domains as the omitted region is homologous between M proteins and cell wall-associated,^{47,48} and alignments were performed using Clustal Omega software.⁴⁹ Primary sequences of M proteins (including site-directed mutant) were arranged into heptad registers using Waggawagga,⁵⁰ a coiled-coil prediction tool paired with a Marcoil algorithm.⁵¹ Established hyaluronic

acid-binding motifs on protein sequences were accumulated from published literature.^{52–54}

2.19 | Statistical analyses

Data are presented as mean \pm standard error of the mean (SEM) of at least three independent experiments. All independent experiments were conducted using three technical replicates and where applicable, plate structure was routinely altered to mitigate positioning bias within data sets. Curve fitting and statistical analyses were conducted using GraphPad Prism 8.4.2 (GraphPad Software, La Jolla, CA). Rate constants (k) for bacterial growth were generated by a nonlinear regression model using the logistic growth equation with least squares fit. All data presented were normally distributed (Shapiro–Wilk) or Log-transformed to conform to normality. For single comparisons, a Student's t -test, with Welch's correction where appropriate, was performed. For multiple comparisons, a one-way analysis of variance with Sidak's post-hoc test was used to determine significant differences. Nonsignificant p values are not shown. Statistical analysis of glycan microarray data has been described previously.¹⁵

3 | RESULTS

3.1 | Phylogenetically diverse M proteins can bind hyaluronic acid with high affinity

To investigate whether phylogenetically diverse M proteins can interact with hyaluronic acid, a comprehensive screen was conducted using glycan microarray technology.⁵⁵ Recombinant M proteins, representative of different *emm* types from 11 major cluster groups and nonclustered M protein (Clade Y, A-C; M57, M14, M19),²² were selected for initial characterization (Table S1). All *emm* cluster groups bound hyaluronic acid (Glycan index 271) or various hyaluronan fragments (Glycan indexes 293–297; 302–313) (Figure 1B), whereby the number of repeating hyaluronan core units D-GlcA- β (1 \rightarrow 3)-D-GlcNAc- β (1 \rightarrow 4) (Table S2) was observed to be a key factor in M protein recognition. To validate the specificity of this interaction, binding to sulfated GAG fragments (Glycan indexes 286–292) was also assessed (Table S2). None of the nonhyaluronic acid structures bound E2 clustered M proteins. Furthermore, nonhyaluronic acid structures demonstrated a reduced capacity to bind different *emm* protein clusters and nonclustered M protein compared to hyaluronic acid structures (Table S3).

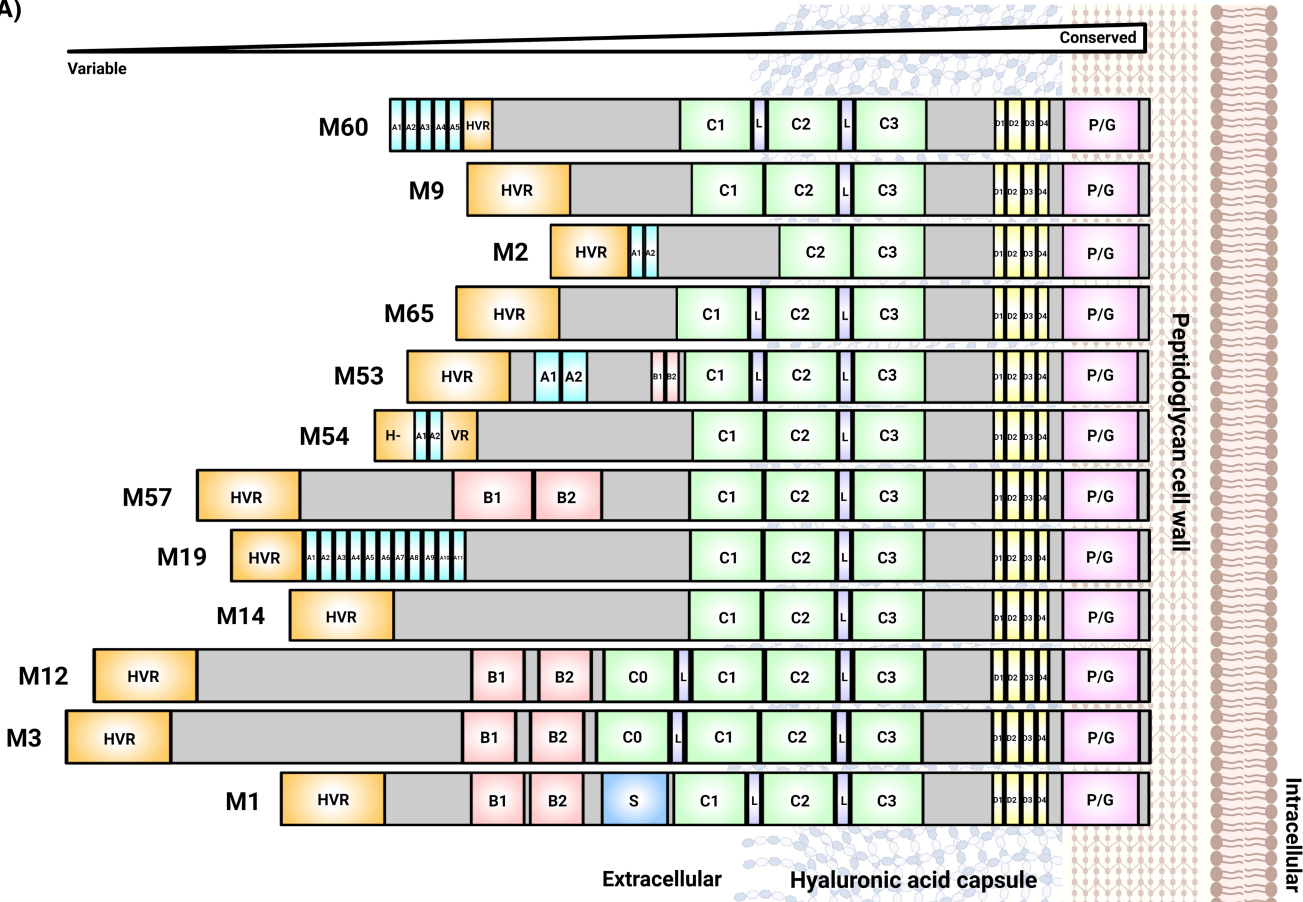
To establish the affinity of M protein–hyaluronic acid interactions, SPR was utilized. His-tagged M proteins (12

from the glycan microarray) were designed to be noncovalently captured on activated NTA sensor chips by their C-terminus to mimic the attachment of M proteins to the GAS surface (Figure 2A). SDS-PAGE analysis of recombinant M proteins revealed bands ranging between 36 and 61 kDa (Figures 2B and S1) corresponding to the expected monomeric size of recombinant M proteins.²² The appearance of doublet bands is typical of recombinant M proteins in *E. coli* expression systems.⁵⁷ Densitometric analysis indicated the relative yield of M protein monomers ranged between 95% and 100% (Table S4), a measure of purity that was optimal for downstream SPR applications. M protein immobilization per cycle was validated by specific positive and negative controls (Figure S2). The binding of hyaluronic acid (25–75 kDa) to recombinant M proteins was assessed using single-cycle kinetics and steady-state affinity analysis was conducted to determine equilibrium dissociation constants for each interaction (K_D). SPR binding analysis revealed that all M proteins tested in this study could interact with increasing concentrations of low molecular weight hyaluronic acid in the designated nanomolar range (Figure 2C), with maximal output responses consistent with previous reports on glycan/GAG–protein interactions using SPR.^{58,59} For some M proteins, affinity constants were determined for each interaction with hyaluronic acid ranging between 66.4 and 195.6 nM (Figures 2D and S3). M proteins for which affinity constants could not be determined (>200 nM) were not further investigated. Collectively, these data indicate that hyaluronic acid may be a conserved ligand for M protein receptors.

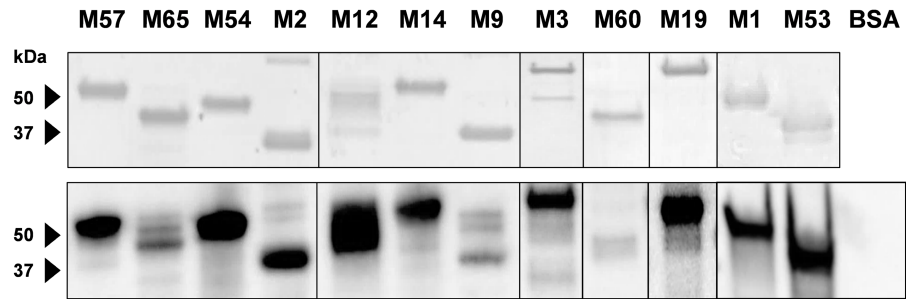
3.2 | Binding of hyaluronic acid is predominately localized to the C repeats of M proteins

To investigate the M protein domains responsible for the interaction with hyaluronic acid, phylogenetically diverse M53 and M1 proteins were selected for truncation mutagenesis. Truncated fragments of M53 and M1 proteins with overlapping repeat domains were designed to localize specific regions responsible for hyaluronic acid recognition, as previously described^{23,60} (Figure 3A). Tris-tricine PAGE analysis of M53 and M1 protein fragments revealed bands ranging between 12–18 and 20–21 kDa, respectively (Figure 3B), which corresponded to the expected sizes of all fragments using the equation for small acidic peptides described previously.⁶¹ Densitometric analysis indicated the relative yield of M protein fragments ranged between 96.3% and 100% (Table S4), a measure of purity that was optimal for downstream SPR applications.

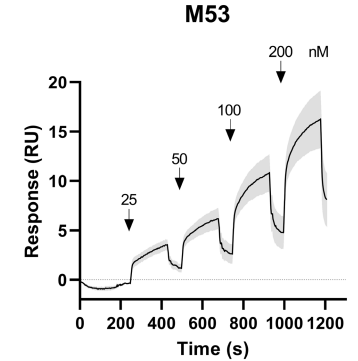
(A)



(B)



(C)



(D)

	A-C pattern					D pattern				E pattern			
	M1	M3	M12	M14	M19	M57	M54	M53	M65	M2	M9	M60	
HA	119.4 ± 4.1	159.2 ± 54.8	195.6 ± 52.6	161.0 ± 12.4	>200	146.8 ± 14.5	>200	159.3 ± 16.8	>200	66.4 ± 39.3	>200	>200	nM

SPR, using single-cycle kinetics, was undertaken to evaluate the binding capabilities of hyaluronic acid to immobilized His-tagged M protein fragments. Hyaluronic acid was demonstrated to bind all M53 protein fragments

with varying affinities (46.2–143.8 nM; or >200 nM) (Figures 3C and S4). Similarly, hyaluronic acid bound the M1 (HVR-B2) fragment with lower affinity (>200 nM) and the M1 (B1–C1) fragment with high affinity (89.9 nM)

FIGURE 2 M proteins bind to hyaluronic acid with high affinity. (A) Schematic of the structural characteristics of M proteins. M proteins are organized by four repeat regions (repeat domains A, B, C, and D) arranged in tandem where the number, size, and amino acid composition of these regions give rise to heterogeneity. Linker (L) regions supporting the C repeat regions may be present. The M1 protein possesses a unique S-region.⁵⁶ The hypervariable region (HVR) lies at the N-terminus exposed to the extracellular environment followed by the variable region in the central region of the M protein which in turn, flanks the highly conserved C-terminus anchored to the peptidoglycan GAS cell wall. Downstream to the D repeats lies the proline/glycine (P/G) rich region with the M protein structures shown above terminating at the LPxTG motif. Visualization was achieved using Illustrator for Biological Sequences and BioRender, where the size of each M protein and the respective domains are to scale, made relative to the number of amino acids present in each sequence. (B) Expression of purified recombinant M proteins (2 μ g or 200 ng) was assessed with Rapid Stain (top panel) and immunoblotting using polyclonal anti-M protein sera (1:30 000) (bottom panel). Bovine serum albumin (BSA) was included as a negative control for sera specificity. (C) Representative sensorgram of hyaluronic acid (HA; 25–200 nM) binding to M proteins using SPR. (D) Affinity constants (nM) for M protein–HA interactions. (C, D) Data shown are mean \pm SEM (or shaded) from three independent experiments.

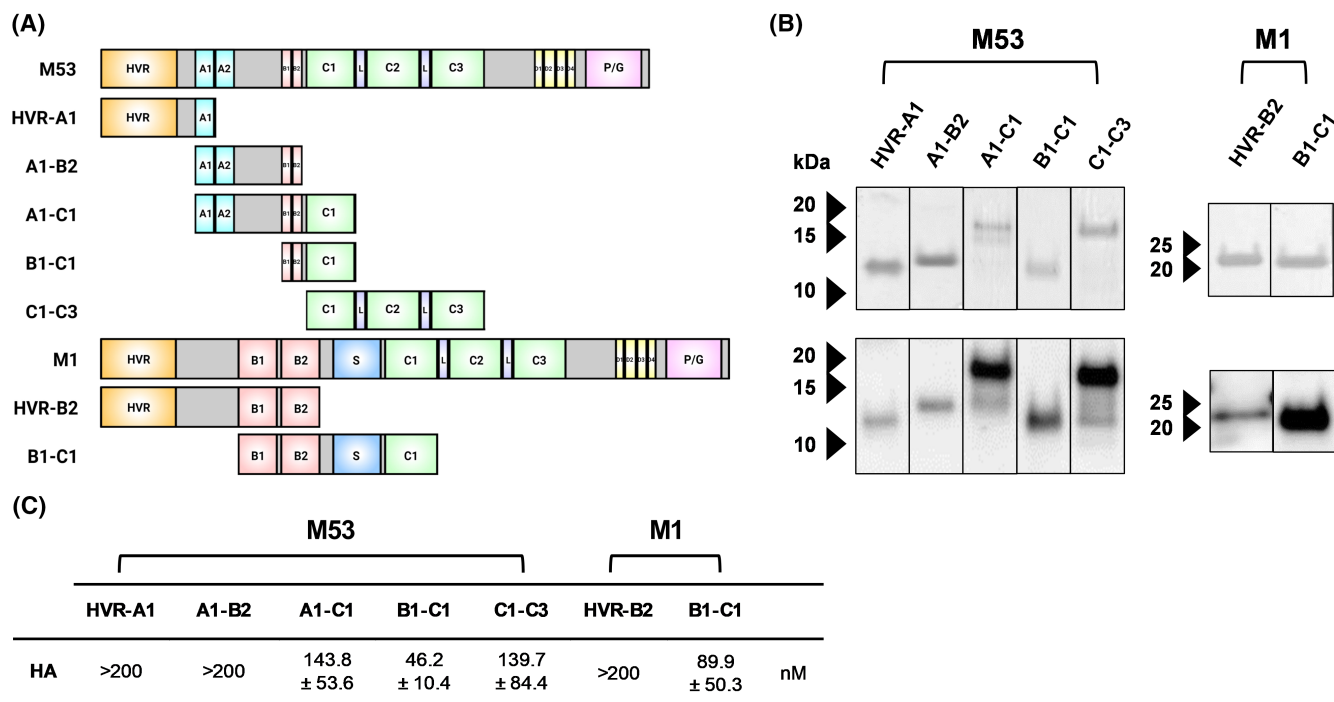


FIGURE 3 Hyaluronic acid binding is localized predominately to the C repeat domain of M proteins. (A) Fragments of M53 and M1 proteins were designed with overlapping repeat domains; see Figure 2 for structural overview. (B) Expression of purified recombinant M protein fragments (2 μ g or 200 ng) was assessed with Colloidal blue stain (top panel) and immunoblotting using polyclonal anti-M protein sera (1:30 000) (bottom panel). (C) Affinity constants (nM) for M protein fragment–hyaluronic acid (HA) interactions using SPR. (B, C) Data shown are representative or mean \pm SEM from three independent experiments.

(Figures 3C and S4). Considering the affinity constants of both M protein fragments and full-length M proteins, these data suggest that multiple M protein domains may facilitate hyaluronic acid binding. Among these binding domains, a shared hyaluronic acid binding motif may be localized to the conserved C repeat region of M proteins.

3.3 | The RR motif in M proteins facilitates binding to hyaluronic acid

It is conceivable that linear hyaluronic acid binding motifs may be conserved between different M proteins.

A previous investigation identified a motif through the generation of a random peptide display library, where sequences containing an arginine–arginine (RR) motif could bind hyaluronic acid.⁵³ This motif was shown to be present in human hyaluronic acid-binding glycoproteins such as CD44.⁵³ Therefore, the presence of this RR motif in M proteins was examined and found to be enriched in the highly conserved C repeat regions of M proteins, corresponding to the SPR findings of full length and M protein fragments described above.

Alignment of the hyaluronic acid-binding domain of CD44 (KNGRYSISR) with full length M protein sequences revealed that the region with the highest

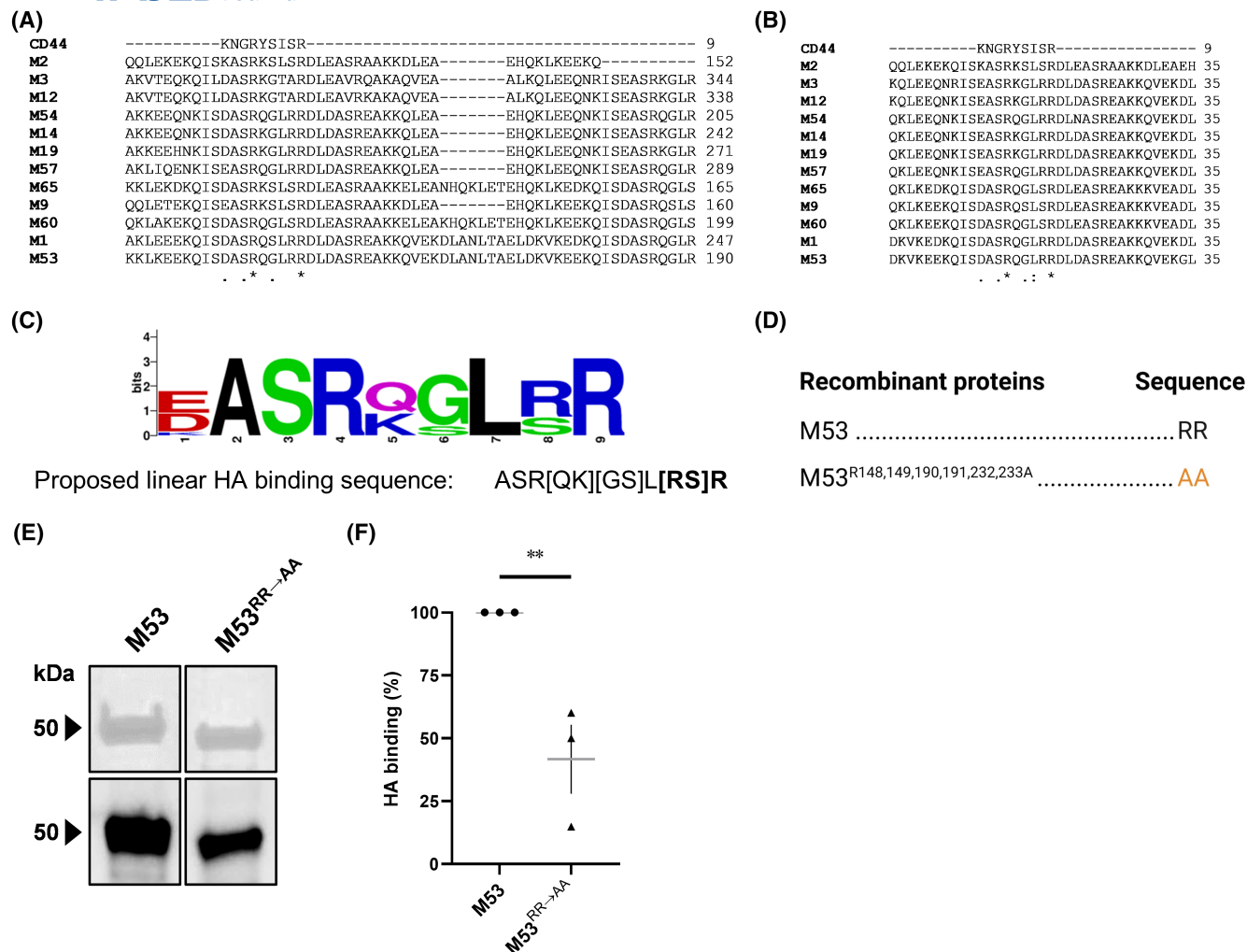


FIGURE 4 Hyaluronic acid binds to M proteins via an RR/SR binding motif. (A) Mature M protein sequences and (B) isolated C2 repeat regions of M proteins were used for alignment with the hyaluronic acid (HA)-binding domain of CD44. (A, B) Asterisk (*) denotes conserved residues; period (.) and colon (:) denote residues that share properties that are weakly or strongly similar, respectively. For the selected regions shown, amino acid positions are indicated on the right. (C) Aligned amino acid residues from the C2 repeat region are represented as a sequence logo leading to a proposed HA binding sequence with the (R/S)R motif in bold. (D) Design of the M53 site-directed protein mutant (M53^{R148,149,190,191,232,233A}; M53^{RR→AA}). Residues of the proposed binding motif were substituted with alanine indicated in orange. (E) Expression of purified recombinant M53^{RR→AA} was assessed with Rapid stain (top panel) and immunoblotting using polyclonal anti-M protein sera (1:30000) (bottom panel). Wild-type M53 protein was included as a positive control. (F) Binding of fluorescein-labeled HA (100 µg/mL) to immobilized M53^{RR→AA} was measured and normalized to wild-type M53 protein. (E, F) Data shown are representative or mean ± SEM from three independent experiments. ***p* < .01 compared to corresponding control (Student's *t*-test).

homology was localized to the C1 or C2 repeats of M proteins (Figure 4A). Moreover, the aligned sequence of M proteins contained the RR motif at its C-terminal (Figure 4A). In some M proteins, the RR motif was substituted with serine-arginine (SR), which is identical to the C-terminal of the CD44 hyaluronic acid-binding domain. Since some M proteins, like M2, do not contain C1 repeats, the KNGRYSISR sequence was then aligned separately with each C repeat from M proteins. The KNGRYSISR sequence shared a higher percent identity with C2 repeats (22.2%–55.6%) (Figure 4B), represented as a sequence logo (Figure 4C). Since the presence of

acidic residues in the first amino acid position of the sequence logo would likely repel electrostatic interactions with the negatively-charged GAG,^{62,63} a refined hyaluronic acid-binding sequence containing the RR/SR motif for M proteins of GAS is proposed (Figure 4C).

M proteins are characterized by their α -helical coiled-coil conformation, facilitated by the arrangement of amino acid residues into heptad registers.^{23,24,60} To confirm the RR/SR motif of the predicted hyaluronic acid-binding sequence is surface-exposed, and therefore available to facilitate GAG interactions, M protein sequences were arranged into heptad registers using a Marcoil algorithm.

The RR/SR motifs found in all C repeats of M proteins are surface-exposed and not buried in the hydrophobic core (Figure S5).

To validate this proposed binding motif in M proteins, site-directed mutagenesis using alanine substitution was implemented based on previous studies.^{64–68} The RR hyaluronic acid-binding motif occurs thrice in the C repeat region of the M53 protein; hence, all six arginine residues were substituted with alanine, with the resulting mutations predicted to not alter the coiled-coil heptad register (Figure 4D). SDS-PAGE analysis revealed a band at 48 kDa, consistent with the expected monomeric size of recombinant M53 protein,²² which was validated using polyclonal anti-M protein sera²⁶ (Figure 4E).

To assess the contribution of RR motifs in M53 protein recognition of hyaluronic acid, a fluorescent plate-based binding assay was implemented whereby 20 µg/mL immobilized wild-type M53 protein and site-directed mutant M53^{R148, 149, 190, 191, 232, 233A} were incubated with 100 µg/mL fluorescein-labeled hyaluronic acid. Binding of hyaluronic acid to M53^{R148, 149, 190, 191, 232, 233A} was significantly reduced by 2.5-fold compared to wild-type M53 protein ($p = .0255$) (Figure 4F). These data indicate a role for the RR motif in the recognition of hyaluronic acid by M53 protein.

3.4 | Recruitment of hyaluronic acid by M proteins decreases wound healing in an M type-specific manner

Since GAS skin infections are typically associated with keratinocyte injury^{69,70} and hyaluronic acid plays integral roles in wound healing,⁷¹ a scratch wound model³⁵ was utilized to investigate the physiological relevance of M protein–hyaluronic acid interactions. First, wound closure was assessed in scratched human HaCaT keratinocytes incubated with 50 µg/mL M53 protein and/or 10 µg/mL hyaluronic acid over 24 h. Incubation with M53 protein or hyaluronic acid alone had minimal effect on wound closure kinetics over time compared to the nil control (Figures 5A and S6A). The lack of effect from hyaluronic acid alone was not unexpected as the mechanism of wound healing in this model is already maximal post-scratching.³⁵ In contrast, co-incubation of M53 protein and hyaluronic acid delayed wound closure over time compared to the nil control (Figures 5A and S6A). This delay over 24 h was significantly different compared to M53 protein ($p = .0358$) and hyaluronic acid alone ($p = .0403$) (Figure 5B). Next, wound closure was assessed in scratched HaCaT keratinocytes incubated with 50 µg/mL M1 protein and/or 10 µg/mL hyaluronic acid over 24 h. M1 protein and hyaluronic acid alone or co-incubated had

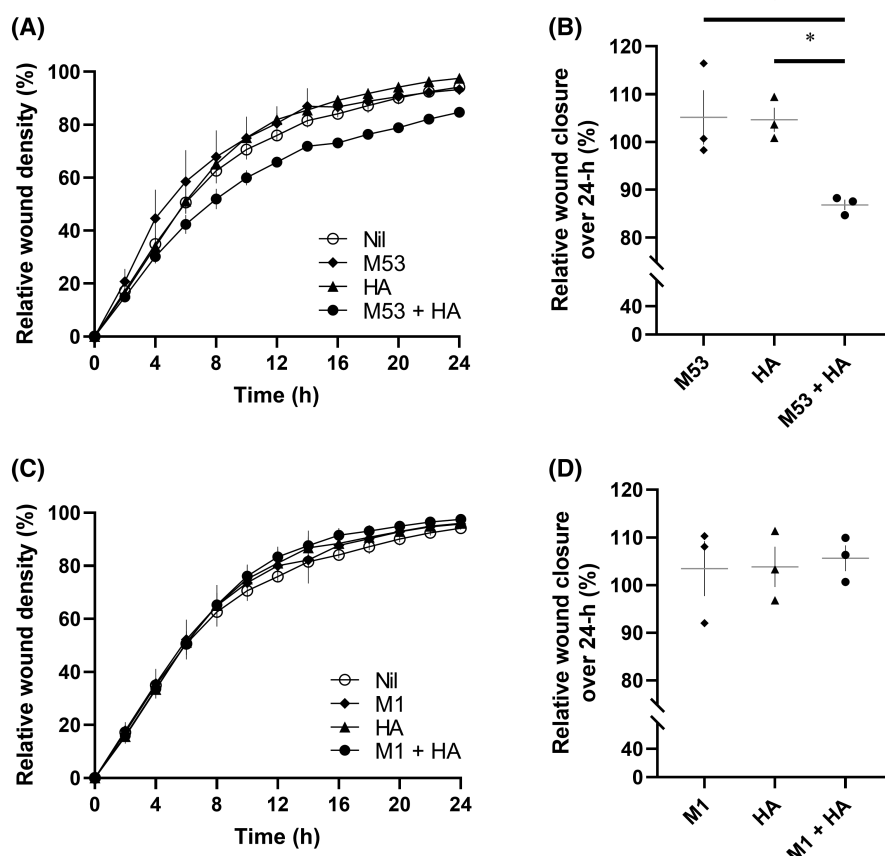


FIGURE 5 M53 proteins but not M1 proteins recruit hyaluronic acid to decrease HaCaT keratinocyte wound healing. (A–D) Scratched HaCaT keratinocytes were incubated in absence (Nil) or presence of (A) M53 proteins or (C) M1 proteins (50 µg/mL) and/or hyaluronic acid (HA; 10 µg/mL) and imaged over 24 h. (A, C) Relative wound density was quantified over time and (B, D) the cumulative responses were normalized to nil. (A–D) Data shown are mean \pm SEM from three independent experiments. (B, D) $*p < .05$ compared to corresponding samples (one-way analysis of variance).

minimal effect on wound closure over time (Figures 5C and 5B) resulting in no significant differences over 24 h ($p = .9327$) (Figure 5D). Collectively, these data indicate that the recruitment of hyaluronic acid to decrease wound healing is an M type-specific function.

3.5 | 5448 and ALAB49 GAS bind hyaluronic acid via M proteins

Next, GAS strains 5448 (A–C pattern, M1) and ALAB49 (D pattern, M53), which produce similar amounts of capsule,^{30,72} were selected to ascertain whether native M proteins function as lectins for hyaluronic acid on a whole cell level. GAS cells were incubated in the absence or presence of 200 $\mu\text{g}/\text{mL}$ fluorescein-labeled hyaluronic acid and interactions were assessed by flow cytometry (Figure 6A). Flow cytometric analysis revealed wild-type GAS isolates 5448 and ALAB49 could bind hyaluronic acid-fluorescein (Figure 6B,C). The fluorescence intensity was greater with wild-type ALAB49 compared to wild-type 5448 (Figure 6B,C), potentially attributable to differences in proteins, glycans or other constituents present on the GAS cell surface between the two strains. Deletion of the *emm* gene encoding M protein, 5448 Δemm1 and ALAB49 Δpam , significantly reduced fluorescence following incubation with hyaluronic acid-fluorescein compared to wild-type 5448 ($p = .0183$) and ALAB49 ($p = .0012$), respectively (Figure 6B,C). Restoration of M protein expression following reverse complementation, 5448 Δemm1 RC and ALAB49 Δpam RC, restored fluorescence levels to

that of the corresponding wild-type 5448 ($p = .9881$) and ALAB49 ($p = .9658$) following incubation with hyaluronic acid-fluorescein (Figure 6B,C). Together, the data suggest that GAS can recruit hyaluronic acid to the cell surface in an M protein-dependent manner.

3.6 | Differences in hyaluronic acid recruitment between 5448 and ALAB49 GAS M protein is not caused by differences in M protein expression

To better understand the differences underlying M protein-mediated hyaluronic acid binding between 5448 and ALAB49 GAS, native M protein expression was investigated. First, *emm1* and *emm53* transcripts at early mid-log growth phase were examined by quantitative PCR. When compared to the GAS housekeeper gene *recA*,⁴⁴ *emm1* mRNA was increased 10-fold while *emm53* mRNA was decreased 10-fold resulting in a 100-fold difference between the two *emm* genes ($p = .0007$) (Figure 7A). To investigate whether this difference correlated to a measurable difference in the amount of M protein, immunoblotting of wild-type 5448 and ALAB49 cell lysates using anti-M protein sera was performed followed by densitometry. Major bands at 53 kDa and 48 kDa were detected for wild-type 5448 and ALAB49, respectively (Figure 7B), corresponding to the expected monomeric size of native M1 and M53 proteins.^{22,73} While the M1 protein expression was increased compared to M53 protein, this difference was not statistically significant relative to total protein ($p = .0517$) (Figure 7C). Isogenic M

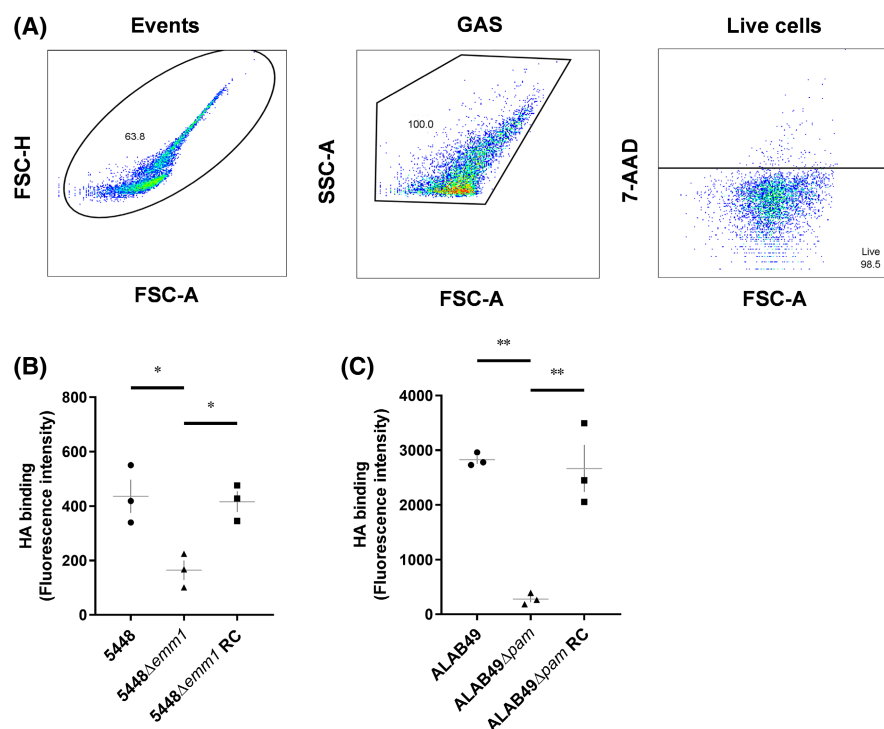


FIGURE 6 5448 and ALAB49 GAS bind hyaluronic acid via M proteins. (A) Flow cytometry gating strategy for the analysis of GAS–hyaluronic acid (HA) interactions. (A–C) Wild-type and mutant (B) 5448-derived and (C) ALAB49-derived GAS strains were pre-treated in the absence or presence of unlabelled HA in 5-fold excess followed by the absence or presence of HA-fluorescein (200 $\mu\text{g}/\text{mL}$) and analyzed via geometric mean fluorescence intensity. Specific GAS–HA interactions are shown, representative or mean \pm SEM from three independent experiments. * $p < .05$ and ** $p < .01$ compared to corresponding samples (one-way analysis of variance).

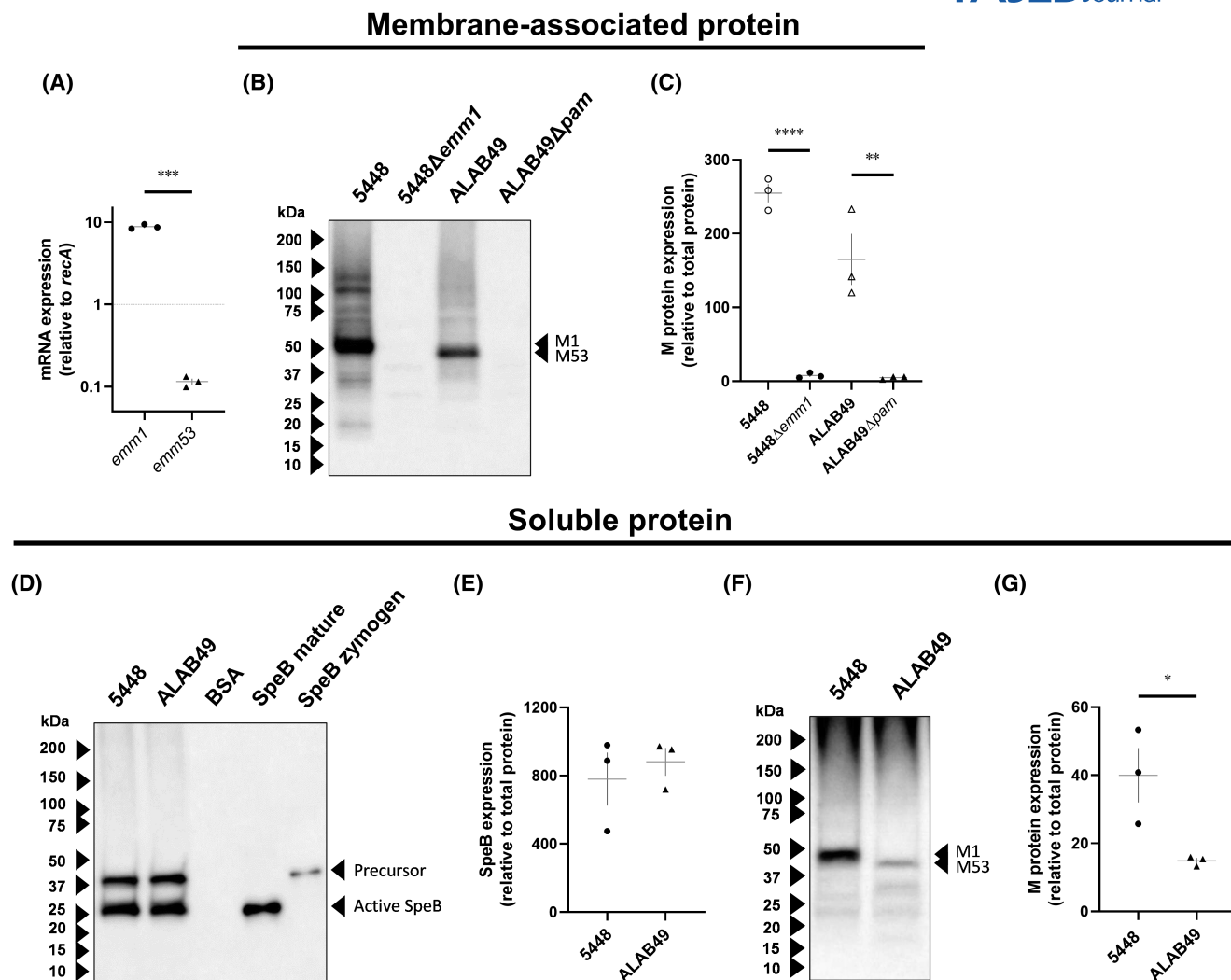


FIGURE 7 mRNA and soluble M protein is significantly increased in 5448 GAS than ALAB49 GAS. (A) M protein gene expression from early mid-log 5448 (*emm1*) and ALAB49 (*emm53*) GAS was assessed by quantitative PCR. (B–C) Expression of cell-associated M proteins (20 µg) from early mid-log wild-type 5448 and ALAB49 GAS and the respective isogenic M protein-deletion mutants was assessed by (B) immunoblotting using polyclonal anti-M protein sera (1:30 000) and (C) quantified using densitometry. (D, E) The presence of SpeB protease (15 µg) from early mid-log GAS supernatants was assessed by (D) immunoblotting and (E) quantified using densitometry. (D) Bovine serum albumin (BSA; 200 ng) was included as a negative control to confirm specificity of polyclonal anti-SpeB sera (1:1000) while purified SpeB proteins (mature and zymogen; 200 ng) were utilized as positive controls. (F, G) Soluble M proteins (15 µg) from early mid-log GAS supernatants were assessed by (F) immunoblotting and (G) quantified using densitometry. (A–G) Data shown are mean ± SEM from three independent experiments. (A, C, E, G) * $p < .05$, ** $p < .01$, *** $p < .001$ and **** $p < .0001$ compared between corresponding samples using (A, E, G) Student's *t*-tests or (C) a one-way analysis of variance.

protein-deletion mutants of 5448 and ALAB49 were also included to confirm the absence of M protein. As expected, no bands corresponding to the monomeric size of M1 or M53 protein were detected in cell lysates from 5448Δ*emm1* and ALAB49Δ*pam* strains, respectively (Figure 7B).

M proteins and other membrane-bound proteins can be released from the GAS surface by proteolytic cleavage,⁷⁴ which may affect GAS–GAG binding. Since this process can be regulated by SpeB activity,⁷⁴ the presence of this virulence factor in GAS supernatants was examined by immunoblotting using anti-SpeB sera followed by

densitometry. Bands at 40 kDa and 27 kDa were detected in wild-type 5448 and ALAB49 supernatants, corresponding to expected sizes of precursor and active SpeB respectively as indicated (Figure 7D).⁷³ There was no significant difference in total secreted SpeB protein expression between the two GAS strains ($p = .2971$) (Figure 7E). Next, amounts of soluble M proteins between GAS strains were assessed. Immunoblotting of 5448 and ALAB49 supernatants with anti-M protein sera revealed major fragments close in size to respective membrane-bound M protein (Figure 7F), corresponding to previous observations.⁷⁵ Densitometric

analysis revealed that soluble M1 protein was significantly increased compared to soluble M53 protein, relative to total protein ($p = .0432$) (Figure 7G). Collectively, these data suggest that the higher level of M protein-dependent hyaluronic acid recruitment reported earlier for ALAB49 GAS compared to 5448 GAS was not due to increased M protein surface expression.

3.7 | Exogenous hyaluronic acid increases 5448 GAS adherence to HaCaT keratinocytes independently of M1 proteins

GAS is known to adhere to skin keratinocytes⁷⁶ via M proteins.⁷⁷ Since host hyaluronic acid is enriched in the skin, an in vitro infection model using HaCaT keratinocytes was employed to examine the effect of exogenous hyaluronic acid on GAS adhesion to host cells. Following pre-incubation of wild-type 5448 with 1 μ M hyaluronic acid, a significant increase in bacterial adherence to HaCaT keratinocytes was observed compared to wild-type 5448 pre-incubated with vehicle ($p = .0499$) (Figure 8A). Analysis of 5448 Δ emm1 following incubation with hyaluronic acid also revealed a significant increase in bacterial adherence to HaCaT keratinocytes compared to 5448 Δ emm1 pre-incubated with vehicle ($p = .0414$) (Figure 8B).

5448 Δ emm1 RC displayed a similar phenotype to wild-type 5448 where bacterial adherence to HaCaT keratinocytes was significantly increased in the presence of hyaluronic acid compared to 5448 Δ emm1 RC pre-incubated with vehicle ($p = .0443$) (Figure 8C). In contrast, pre-incubation of wild-type ALAB49 with hyaluronic acid revealed no significant difference in bacterial adherence to HaCaT keratinocytes compared to wild-type ALAB49 pre-incubated with vehicle ($p = .4429$) (Figure 8D).

To confirm that hyaluronic acid was not affecting bacterial growth over the course of HaCaT keratinocyte infection, growth kinetics of wild-type 5448 and ALAB49 were assessed in the presence of 1 μ M hyaluronic acid. In the presence of hyaluronic acid, wild-type 5448 and ALAB49 revealed similar growth profiles to corresponding GAS incubated with vehicle (Figure S7A,C), with no significant differences in growth rate ($p = .1482$ and $p = .4948$, respectively; Figure S7B,D). This suggests that the observed increase in 5448 GAS adherence mediated by hyaluronic acid was not due to increased bacterial growth in the presence of this GAG. To confirm that exogenous hyaluronic acid was not affecting bacterial autoaggregation over the course of HaCaT keratinocyte infection, the sedimentation of wild-type 5448 and ALAB49 was monitored over time in the presence of 500 μ g/mL hyaluronic acid. Wild-type 5448 and ALAB49 GAS showed similar aggregation profiles over time which was not modified in the presence

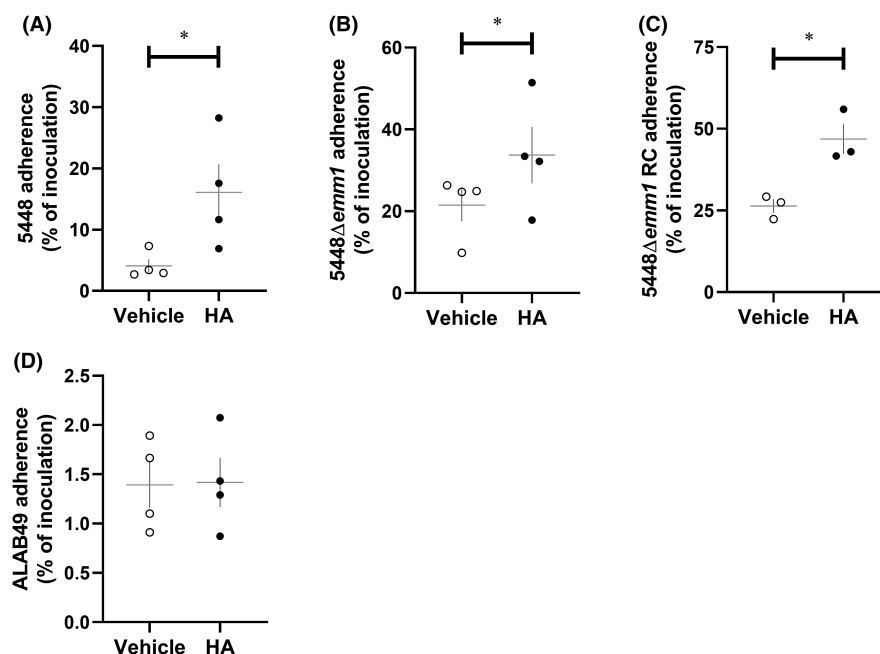


FIGURE 8 Hyaluronic acid increases 5448 GAS adherence to HaCaT keratinocytes independently of M1 proteins. (A–C) Wild-type and mutant 5448-derived GAS strains or (D) wild-type ALAB49 GAS were pre-incubated with hyaluronic acid (HA; 1 μ M) or corresponding vehicle prior to infection with HaCaT keratinocytes at a MOI of 5:1 GAS:HaCaT. Bacterial adherence (%) was determined by enumeration of recovered bacteria relative to the original inoculum. (A–D) Data shown are mean \pm SEM from (C) three or (A, B, D) four independent experiments. * $p < .05$ compared to corresponding control (Student's t -test).

of hyaluronic acid compared to corresponding vehicle ($p = .5664$) (Figure S7E). Collectively, these data suggest hyaluronic acid can increase 5448, but not ALAB49, GAS adherence to HaCaT keratinocytes independently of M protein interactions.

4 | DISCUSSION

While GAS has been previously demonstrated to bind a subset of GAGs, evidence for the participation of M proteins functioning as a surface-expressed lectin of GAS to mediate host GAG interactions is limited. The purpose of this study was to identify and functionally characterize the interaction between host hyaluronic acid and M proteins. High affinity interaction with hyaluronic acid was shown to be conserved across phylogenetically diverse M proteins, mediated by RR/SR motifs localized in the C repeat region. The recruitment of hyaluronic acid by M proteins to decrease host wound healing was M type-specific, and whole cell GAS were also shown to bind hyaluronic acid via M proteins.

Hyaluronic acid was found to bind all M proteins utilized in this study. A major reservoir for this GAG is the skin.^{78–80} Healthy skin surfaces typically maintain a pH range of 4.2–5.6, with a gradient down the epidermis to a neutral pH.⁸¹ Previous work investigating hyaluronic acid binding interactions using SPR demonstrated a pH-dependent relationship with an inflammatory human host protein where binding was observed under acidic conditions,⁸² contrasting to the neutral pH (7.4) utilized in the current study. Skin trauma, which is characteristic of GAS infection,⁹ can shift the environmental pH to neutral—alkaline (average 7.4) conditions,⁸³ and it is known that bacterial colonization increases in alkaline environments.⁸⁴ Since hyaluronic acid associates noncovalently with proteoglycans,⁸⁵ hyaluronic acid chains may detach from host proteoglycans under these environmental conditions, enabling M proteins to bind to hyaluronic acid during infection. Moreover, host wound beds are enriched with GAGs,⁷⁸ and hyaluronic acid can regulate wound healing.²⁰ Therefore, it is conceivable that the recruitment of GAGs to the GAS surface by M protein-mediated interactions may dampen the immune response. This is further supported by our observations where M53 proteins of a skin-tropic strain, but not M1 proteins of a throat-tropic strain, could recruit exogenous hyaluronic acid to decrease keratinocyte wound healing; a divergence in function which may stem from differences in molecular pathogenesis underlying tissue tropism. While M1 and M53 proteins can readily bind hyaluronic acid with similar affinity, the capacity to form complexes in solution compared to a stable attachment at the SPR chip surface,⁸⁶ or with other

ECM constituents in a wound-healing environment due to the structural variation at the N-terminus, may underlie the observed differences in the effect of these proteins on the wound healing response. It remains to be determined if the differences reported here also occur on a whole cell level using a more physiologically-relevant model of GAS skin infection.

Discrete M protein domains were shown to facilitate hyaluronic acid interactions which led to the proposal of a linear RR/SR sequence motif in the C repeat region, consistent with other M protein-mediated interactions with GAGs.¹⁷ This study represents the first examination of the contribution of the RR motif in full length M proteins to hyaluronic acid binding interactions. Although all GAGs are negatively charged and predominately bind to proteins via ionic interactions with basic residues,⁸⁷ the specificity of the RR motif has been previously investigated, revealing that other GAG subclasses, such as chondroitin sulfate and heparan sulfate, do not interact with this motif.⁵³ Hyaluronic acid is the only GAG that is nonsulfated,⁸⁸ increasing the number of hydrogen bonds within the GAG structure (Figure 1A). Recent evidence suggests the strength of the hydrogen bond at the glycosidic linker regions contributes to the structural flexibility of hyaluronic acid at longer disaccharide chain lengths,⁸⁹ including the low molecular weight hyaluronic acid used for SPR binding interactions. Hence, hyaluronic acid may adopt a more favorable conformation that enables two adjacent carboxyl groups to align with the RR sequence compared to other GAGs, as previously suggested.⁵³ Although a primary linear motif was proposed in this study, it is likely that accessory interactions with polar or uncharged residues spanning the protein backbone would further cement hyaluronic acid interactions. This is supported by the finding that hyaluronic acid binding was not completely abolished by mutagenesis of the RR motifs present in M53 protein, as well as affinity constants determined for M53 protein fragments lacking the C repeat region.

Having demonstrated that M proteins can bind host hyaluronic acid, it also raises the possibility that M proteins can also recognize GAS capsular hyaluronic acid, potentially impacting bacterial aggregation, biofilm formation, and host immune evasion mechanisms. The endogenous hyaluronic acid bacterial capsule is a known modulator of GAS adherence and colonization^{32,90–92} with antiphagocytic^{93–96} and antioxidant⁹⁷ functions. To date, little is known about how the capsule is biochemically anchored to the GAS surface; the RR sequences on M proteins may underlie this mechanism, and this warrants further investigation. Recent findings suggest the upregulation of hyaluronic acid capsule also plays a role in mediating bacterial aggregation as a noncanonical mechanism for biofilm formation on abiotic surfaces.⁹⁸ Whether M proteins

function synergistically with the capsule in this process is the focus of ongoing investigations.

Building on the work of Frick et al.¹⁷, the data presented in this study indicate that GAS can recruit hyaluronic acid in an M protein-dependent manner. Notably, ALAB49 GAS demonstrated a greater capacity to bind hyaluronic acid than 5448 GAS, a difference that appeared to correlate with the presence of their respective M proteins despite no difference in native M protein surface expression. Whole cell binding analysis was conducted at a temperature supporting M protein dimer formation,²⁴ a conformation known to stabilize ligand interactions and promote higher affinity interactions with secondary protein ligands.^{99,100} If more binding sites for hyaluronic acid exist within M53 protein than M1 protein, M protein dimerization may facilitate enhanced binding of hyaluronic acid for ALAB49 compared to 5448 GAS. Hence, the stoichiometry of binding, or the ability to form complexes between M proteins and GAGs, may explain differences in hyaluronic acid binding observed for these two strains. Different GAS strains express a diverse set of adhesins,¹⁰¹ and strain-dependent or *emm* pattern-specific interactions with host proteins have been extensively recognized.²² ALAB49 GAS, derived from a skin impetigo infection,^{29,30} and 5448 GAS, isolated from an invasive soft tissue infection,^{27,102} exhibit distinct tissue tropisms. Given host hyaluronic acid is abundant in the skin,^{78–80} the enhanced binding propensity of ALAB49 to this GAG compared to 5448 GAS may be associated with tissue tropism. Moreover, invasive clinical strains of GAS have been previously profiled to have decreased adherence capabilities, partially attributable to decreased adhesin expression.^{103,104} It is conceivable that ALAB49 GAS may express an increased number of potential hyaluronic acid-binding receptors on the bacterial surface.

While no difference in surface-expressed M protein levels was observed between ALAB49 and 5448 GAS, the amount of soluble M protein in GAS supernatants was higher for 5448 than ALAB49. GAS secrete proteases such as SpeB that can liberate M proteins from the surface,^{74,105} and soluble M proteins can function as potent T-cell activators that exacerbate host cell inflammation, a key characteristic of invasive GAS infections.¹⁰⁶ While SpeB is highly conserved¹⁰⁷ and is reported to be functionally active in both 5448¹⁰⁸ and ALAB49 GAS,¹⁰⁹ a number of genes are implicated in altered SpeB protease activity and disruptions to these components directly affect SpeB production.¹¹⁰ Here, comparable amounts of SpeB between 5448 and ALAB49 GAS were detected, and it is therefore unlikely increased soluble M protein was due to increased protease activity. The increased removal of M1 protein from the 5448 GAS cell surface may explain the increased level of *emm1* transcripts, driving a compensatory

mechanism to restore surface-bound M protein. Since native surface M protein expression was consistent between 5448 and ALAB49 GAS, it reinforces that the differences in hyaluronic acid recruitment between the two strains may be due to differences in avidity or multivalent interactions between M proteins and hyaluronic acid.

Unlike ALAB49 GAS, the adherence of 5448 GAS to HaCaT keratinocytes was increased in the presence of hyaluronic acid. It is known that *emm* pattern-predicted tissue tropism does not correlate with a preferential ability to adhere to specific immortalized cell lines in vitro.¹¹¹ The observed increase in adherence in this study suggests a mode of adherence known as bridging,¹⁰¹ where hyaluronic acid may act as a linker module between GAS and HaCaT keratinocytes. Hyaluronic acid increased 5448 GAS adherence independently of M1 protein expression, indicating the contribution of additional surface-expressed receptors involved in the recognition of hyaluronic acid by 5448 GAS. It is known that the hyaluronic acid capsule of GAS can facilitate bacterial adherence to keratinocytes via CD44 receptor-mediated signaling.⁹¹ Since homologous glycan–glycan interactions have been reported in eukaryotes with functions in adhesion events,^{112–115} it is possible that GAS capsular hyaluronic acid may also engage in homologous binding interactions with exogenous hyaluronic acid to serve as a linker module to host cell surface components. Alternatively, it is well known that capsular hyaluronic acid can physically block M protein-mediated interactions in a cell- and strain-specific manner.^{77,116–118} Since M proteins can bind to host hyaluronic acid via the C repeat region close to the GAS surface, it is also possible that endogenous expression of hyaluronic acid by GAS may negate any M protein-mediated effects of exogenous hyaluronic acid or mask M protein interactions with keratinocytes. In vivo, homologous interactions of hyaluronic acid may directly facilitate bacterial adherence for initial GAS colonization, while M protein-mediated interactions with host hyaluronic acid may occur under selective environmental pressures that decrease GAS capsule production¹¹⁹ or by soluble M proteins to trap pro-inflammatory low molecular weight hyaluronic acid to prevent bacterial clearance.²¹

Collectively, this study presents an alternative mechanism for GAS colonization and adherence to human host cells through the acquisition of hyaluronic acid. An enhanced understanding of M protein-mediated delays in host wound healing may contribute to the development of novel therapeutics that arrest disease progression, and warrants further investigation.

AUTHOR CONTRIBUTIONS

All authors have read and approved the final manuscript. Tahnee B.-D. McEwan (Conceptualization, investigation,

methodology, formal analysis, writing—original draft, and visualization); David M. P. De Oliveira (Investigation, formal analysis, methodology, resources); Emily K. Stares (Investigation, formal analysis); Lauren E. Hartley-Tassell (Investigation, methodology); Christopher J. Day (Investigation, methodology); Emma-Jayne Proctor (Methodology); Victor Nizet (Conceptualization and resources); Mark J. Walker (Conceptualization, resources); Michael P. Jennings (Conceptualization, funding acquisition, methodology, and resources); Ronald Sluyter (Conceptualization, methodology, validation, supervision, resources, writing—review and editing); Martina L. Sanderson-Smith (Conceptualization, investigation, funding acquisition, methodology, validation, project administration, supervision, resources, writing—review and editing).

ACKNOWLEDGMENTS

The authors thank the staff of Molecular Horizons and the Fluorescence Analysis Facility (University of Wollongong) for technical assistance.

FUNDING INFORMATION

This project was supported by the National Health and Medical Research Council (Project Grant APP1143266 and Principal Research Fellowship 1138466 to MLS-S and MPJ, respectively).


DISCLOSURES

The authors declare no conflict of interest.


DATA AVAILABILITY STATEMENT

The data that support the findings of this study are available on request from the corresponding author. The data are not publicly available due to privacy or ethical restrictions.

ORCID

Tahnee B.-D. McEwan  <https://orcid.org/0000-0002-9619-414X>

David M. P. De Oliveira  <https://orcid.org/0000-0002-5085-7163>

Lauren E. Hartley-Tassell  <https://orcid.org/0000-0003-2415-0321>

Christopher J. Day  <https://orcid.org/0000-0001-7953-4408>

Emma-Jayne Proctor  <https://orcid.org/0000-0002-9229-7694>

Victor Nizet  <https://orcid.org/0000-0003-3847-0422>

Mark J. Walker  <https://orcid.org/0000-0001-7423-2769>

Michael P. Jennings  <https://orcid.org/0000-0002-1027-4684>

Ronald Sluyter  <https://orcid.org/0000-0003-4909-686X>

Martina L. Sanderson-Smith  <https://orcid.org/0000-0002-6366-4993>

REFERENCES

- Ikuta KS, Swetschinski LR, Robles Aguilar G, et al. Global mortality associated with 33 bacterial pathogens in 2019: a systematic analysis for the Global Burden of Disease Study 2019. *Lancet*. 2023;400:2221-2248.
- Walker MJ, Barnett TC, McArthur JD, et al. Disease manifestations and pathogenic mechanisms of group A *Streptococcus*. *Clin Microbiol Rev*. 2014;27:264-301.
- Barnett TC, Bowen AC, Carapetis JR. The fall and rise of group A *Streptococcus* diseases. *Epidemiol Infect*. 2018;147:e4.
- Courtney HS, Hasty DL, Dale JB. Molecular mechanisms of adhesion, colonization, and invasion of group A *Streptococci*. *Ann Med*. 2002;34:77-87.
- Kapur V, Topouzis S, Majesky MW, et al. A conserved *Streptococcus pyogenes* extracellular cysteine protease cleaves human fibronectin and degrades vitronectin. *Microb Pathog*. 1993;15:327-346.
- Lottenberg R, DesJardin LE, Wang H, Boyle MD. Streptokinase-producing *Streptococci* grown in human plasma acquire unregulated cell-associated plasmin activity. *J Infect Dis*. 1992;166:436-440.
- Khil J, Im M, Heath A, et al. Plasminogen enhances virulence of group A *Streptococci* by streptokinase-dependent and streptokinase-independent mechanisms. *J Infect Dis*. 2003;188:497-505.
- Singh B, Fleury C, Jalalvand F, Riesbeck K. Human pathogens utilize host extracellular matrix proteins laminin and collagen for adhesion and invasion of the host. *FEMS Microbiol Rev*. 2012;36:1122-1180.
- Brouwer S, Rivera-Hernandez T, Curren BF, et al. Pathogenesis, epidemiology and control of group A *Streptococcus* infection. *Nat Rev Microbiol*. 2023;21:431-447.
- Lindsay S, Oates A, Bourdillon K. The detrimental impact of extracellular bacterial proteases on wound healing. *Int Wound J*. 2017;14:1237-1247.
- Vu HM, Hammers DE, Liang Z, et al. Group A *Streptococcus*-induced activation of human plasminogen is required for keratinocyte wound retraction and rapid clot dissolution. *Front Cardiovasc Med*. 2021;8:667554.
- McEwan TB, Sanderson-Smith ML, Sluyter R. Purinergic signalling in group A *Streptococcus* pathogenesis. *Front Immunol*. 2022;13:872053.
- Johnson AF, LaRock CN. Antibiotic treatment, mechanisms for failure, and adjunctive therapies for infections by group A *Streptococcus*. *Front Microbiol*. 2021;12:760255.
- Sanderson-Smith ML, Dinkla K, Cole JN, et al. M protein-mediated plasminogen binding is essential for the virulence of an invasive *Streptococcus pyogenes* isolate. *FASEB J*. 2008;22:2715-2722.
- De Oliveira DM, Hartley-Tassell L, Everest-Dass A, et al. Blood group antigen recognition via the group A *Streptococcal* M protein mediates host colonization. *MBio*. 2017;8:e02237-16.
- De Oliveira DMP, Everest-Dass A, Hartley-Tassell L, et al. Human glycan expression patterns influence group A *Streptococcal* colonization of epithelial cells. *FASEB J*. 2019;33:10808-10818.
- Frick IM, Schmidtchen A, Sjöbring U. Interactions between M proteins of *Streptococcus pyogenes* and glycosaminoglycans

- promote bacterial adhesion to host cells. *Eur J Biochem.* 2003;270:2303-2311.
18. Fraser JR, Laurent TC, Laurent UB. Hyaluronan: its nature, distribution, functions and turnover. *J Intern Med.* 1997;242:27-33.
 19. Gandhi NS, Mancera RL. The structure of glycosaminoglycans and their interactions with proteins. *Chem Biol Drug Des.* 2008;72:455-482.
 20. Papakonstantinou E, Roth M, Karakiulakis G. Hyaluronic acid: a key molecule in skin aging. *Dermatoendocrinol.* 2012;4:253-258.
 21. Schommer NN, Muto J, Nizet V, Gallo RL. Hyaluronan breakdown contributes to immune defense against group A *Streptococcus*. *J Biol Chem.* 2014;289:26914-26921.
 22. Sanderson-Smith M, De Oliveira DM, Guglielmini J, et al. A systematic and functional classification of *Streptococcus pyogenes* that serves as a new tool for molecular typing and vaccine development. *J Infect Dis.* 2014;210:1325-1338.
 23. McNamara C, Zinkernagel AS, Macheboeuf P, Cunningham MW, Nizet V, Ghosh P. Coiled-coil irregularities and instabilities in group A *Streptococcus* M1 are required for virulence. *Science.* 2008;319:1405-1408.
 24. Nilson BH, Frick IM, Akesson P, et al. Structure and stability of protein H and the M1 protein from *Streptococcus pyogenes*. Implications for other surface proteins of gram-positive bacteria. *Biochemistry.* 1995;34:13688-13698.
 25. Berge A, Sjöbring U. PAM, a novel plasminogen-binding protein from *Streptococcus pyogenes*. *J Biol Chem.* 1993;268:25417-25424.
 26. Sanderson-Smith M, Batzloff M, Sriprakash KS, Dowton M, Ranson M, Walker MJ. Divergence in the plasminogen-binding group A *Streptococcal* M protein family: functional conservation of binding site and potential role for immune selection of variants. *J Biol Chem.* 2006;281:3217-3226.
 27. Aziz RK, Pabst MJ, Jeng A, et al. Invasive M1T1 group A *Streptococcus* undergoes a phase-shift in vivo to prevent proteolytic degradation of multiple virulence factors by SpeB. *Mol Microbiol.* 2004;51:123-134.
 28. Kansal RG, McGeer A, Low DE, Norrby-Teglund A, Kotb M. Inverse relation between disease severity and expression of the *Streptococcal* cysteine protease, SpeB, among clonal M1T1 isolates recovered from invasive group A *Streptococcal* infection cases. *Infect Immun.* 2000;68:6362-6369.
 29. Enright MC, Spratt BG, Kalia A, Cross JH, Bessen DE. Multilocus sequence typing of *Streptococcus pyogenes* and the relationships between emm type and clone. *Infect Immun.* 2001;69:2416-2427.
 30. Svensson MD, Sjöbring U, Luo F, Bessen DE. Roles of the plasminogen activator streptokinase and the plasminogen-associated M protein in an experimental model for *Streptococcal* impetigo. *Microbiology (Reading).* 2002;148:3933-3945.
 31. Lauth X, von Kückritz-Blickwede M, McNamara CW, et al. M1 protein allows group A *Streptococcal* survival in phagocyte extracellular traps through cathelicidin inhibition. *J Innate Immun.* 2009;1:202-214.
 32. Hollands A, Pence MA, Timmer AM, et al. Genetic switch to hypervirulence reduces colonization phenotypes of the globally disseminated group A *Streptococcus* M1T1 clone. *J Infect Dis.* 2010;202:11-19.
 33. Ji Y, Schnitzler N, DeMaster E, Cleary P. Impact of M49, Mrp, Enn, and C5a peptidase proteins on colonization of the mouse oral mucosa by *Streptococcus pyogenes*. *Infect Immun.* 1998;66:5399-5405.
 34. Dorken G, Ferguson GP, French CE, Poon WC. Aggregation by depletion attraction in cultures of bacteria producing exopolysaccharide. *J R Soc Interface.* 2012;9:3490-3502.
 35. McEwan TB, Sophocleous RA, Cuthbertson P, Mansfield KJ, Sanderson-Smith ML, Sluyter R. Autocrine regulation of wound healing by ATP release and P2Y(2) receptor activation. *Life Sci.* 2021;283:119850.
 36. Dabbs RA, Wilson MR. Expression and purification of chaperone-active recombinant clusterin. *PLoS One.* 2014;9:e86989.
 37. Bray L, Froment C, Pardo P, et al. Identification and functional characterization of the phosphorylation sites of the neuropeptide FF2 receptor. *J Biol Chem.* 2014;289:33754-33766.
 38. Williams JG, Ly D, Geraghty NJ, et al. *Streptococcus pyogenes* M1T1 variants induce an inflammatory neutrophil phenotype including activation of inflammatory caspases. *Front Cell Infect Microbiol.* 2020;10:596023.
 39. Han S, Cui Y, Helbing DL. Inactivation of horseradish peroxidase by acid for sequential chemiluminescent western blot. *Biotechnol J.* 2020;15:e1900397.
 40. Roberts JJ, Elder RM, Neumann AJ, Jayaraman A, Bryant SJ. Interaction of hyaluronan binding peptides with glycosaminoglycans in poly(ethylene glycol) hydrogels. *Biomacromolecules.* 2014;15:1132-1141.
 41. Nieba L, Nieba-Axmann SE, Persson A, et al. BIACORE analysis of histidine-tagged proteins using a chelating NTA sensor chip. *Anal Biochem.* 1997;252:217-228.
 42. Xiao C-Q, Huang Q, Zhang Y, Zhang H-Q, Lai L. Binding thermodynamics of divalent metal ions to several biological buffers. *Thermochim Acta.* 2020;691:178721.
 43. O'Shannessy DJ, Brigham-Burke M, Sonesson KK, Hensley P, Brooks I. Determination of rate and equilibrium binding constants for macromolecular interactions using surface plasmon resonance: use of nonlinear least squares analysis methods. *Anal Biochem.* 1993;212:457-468.
 44. Frost HR, Davies MR, Delforge V, et al. Analysis of global collection of group A *Streptococcus* genomes reveals that the majority encode a trio of M and M-Like proteins. *mSphere.* 2020;5:e00806-19.
 45. Livak KJ, Schmittgen TD. Analysis of relative gene expression data using real-time quantitative PCR and the 2^{-ΔΔCT} Method. *Methods.* 2001;25:402-408.
 46. Rao X, Huang X, Zhou Z, Lin X. An improvement of the 2^{-ΔΔCT} method for quantitative real-time polymerase chain reaction data analysis. *Biostat Bioinforma Biomath.* 2013;3:71-85.
 47. Fischetti VA. *Streptococcal* M protein: molecular design and biological behavior. *Clin Microbiol Rev.* 1989;2:285-314.
 48. Azuar A, Jin W, Mukaida S, Hussein WM, Toth I, Skwarczynski M. Recent advances in the development of peptide vaccines and their delivery systems against group A *Streptococcus*. *Vaccines (Basel).* 2019;7:58.
 49. Madeira F, Pearce M, Tivey ARN, et al. Search and sequence analysis tools services from EMBL-EBI in 2022. *Nucleic Acids Res.* 2022;50:W276-W279.
 50. Simm D, Hatje K, Kollmar M. Waggawagga: comparative visualization of coiled-coil predictions and detection of stable single α-helices (SAH domains). *Bioinformatics.* 2015;31:767-769.

51. Delorenzi M, Speed T. An HMM model for coiled-coil domains and a comparison with PSSM-based predictions. *Bioinformatics*. 2002;18:617-625.
52. Yang B, Yang BL, Savani RC, Turley EA. Identification of a common hyaluronan binding motif in the hyaluronan binding proteins RHAMM, CD44 and link protein. *EMBO J*. 1994;13:286-296.
53. Amemiya K, Nakatani T, Saito A, Suzuki A, Munakata H. Hyaluronan-binding motif identified by panning a random peptide display library. *Biochim Biophys Acta*. 2005;1724:94-99.
54. Dicker KT, Gurski LA, Pradhan-Bhatt S, Witt RL, Farach-Carson MC, Jia X. Hyaluronan: a simple polysaccharide with diverse biological functions. *Acta Biomater*. 2014;10:1558-1570.
55. Day CJ, Tiralongo J, Hartnell RD, et al. Differential carbohydrate recognition by *Campylobacter jejuni* strain 11168: influences of temperature and growth conditions. *PLoS One*. 2009;4:e4927.
56. Akesson P, Schmidt KH, Cooney J, Björck L. M1 protein and protein H: IgGFC- and albumin-binding *Streptococcal* surface proteins encoded by adjacent genes. *Biochem J*. 1994;300(Pt 3):877-886.
57. Gustafsson MC, Lannergård J, Nilsson OR, et al. Factor H binds to the hypervariable region of many *Streptococcus pyogenes* M proteins but does not promote phagocytosis resistance or acute virulence. *PLoS Pathog*. 2013;9:e1003323.
58. Munakata H, Takagaki K, Majima M, Endo M. Interaction between collagens and glycosaminoglycans investigated using a surface plasmon resonance biosensor. *Glycobiology*. 1999;9:1023-1027.
59. Day CJ, Röltgen K, Pluschke G, Jennings MP. The cell surface protein MUL_3720 confers binding of the skin pathogen *Mycobacterium ulcerans* to sulfated glycans and keratin. *PLoS Negl Trop Dis*. 2021;15:e0009136.
60. Macheboeuf P, Buffalo C, Fu CY, et al. *Streptococcal* M1 protein constructs a pathological host fibrinogen network. *Nature*. 2011;472:64-68.
61. Guan Y, Zhu Q, Huang D, Zhao S, Jan Lo L, Peng J. An equation to estimate the difference between theoretically predicted and SDS PAGE-displayed molecular weights for an acidic peptide. *Sci Rep*. 2015;5:13370.
62. Marcisz M, Zacharias M, Samsonov SA. Modeling protein-glycosaminoglycan complexes: does the size matter? *J Chem Inf Model*. 2021;61:4475-4485.
63. Shi D, Sheng A, Chi L. Glycosaminoglycan-protein interactions and their roles in human disease. *Front Mol Biosci*. 2021;8:639666.
64. Delacoux F, Fichard A, Cogne S, Garrone R, Ruggiero F. Unraveling the amino acid sequence crucial for heparin binding to collagen V. *J Biol Chem*. 2000;275:29377-29382.
65. Mahoney DJ, Blundell CD, Day AJ. Mapping the hyaluronan-binding site on the link module from human tumor necrosis factor-stimulated gene-6 by site-directed mutagenesis. *J Biol Chem*. 2001;276:22764-22771.
66. Proudfoot AE, Fritchley S, Borlat F, et al. The BBXB motif of RANTES is the principal site for heparin binding and controls receptor selectivity. *J Biol Chem*. 2001;276:10620-10626.
67. Peterson FC, Elgin ES, Nelson TJ, et al. Identification and characterization of a glycosaminoglycan recognition element of the C chemokine lymphotactin. *J Biol Chem*. 2004;279:12598-12604.
68. Kattamuri C, Nolan K, Thompson TB. Analysis and identification of the Grem2 heparin/heparan sulfate-binding motif. *Biochem J*. 2017;474:1093-1107.
69. Wang B, Ruiz N, Pentland A, Caparon M. Keratinocyte proinflammatory responses to adherent and nonadherent group A *Streptococci*. *Infect Immun*. 1997;65:2119-2126.
70. Scaramuzzino DA, McNiff JM, Bessen DE. Humanized in vivo model for *Streptococcal* impetigo. *Infect Immun*. 2000;68:2880-2887.
71. Melrose J. Glycosaminoglycans in wound healing. *Bone Tissue Regen Insights*. 2016;7:BTRI.S38670.
72. Maamary PG, Sanderson-Smith ML, Aziz RK, et al. Parameters governing invasive disease propensity of non-M1 serotype group A *Streptococci*. *J Innate Immun*. 2010;2:596-606.
73. Cole JN, McArthur JD, McKay FC, et al. Trigger for group A *Streptococcal* M1T1 invasive disease. *FASEB J*. 2006;20:1745-1747.
74. Berge A, Björck L. Streptococcal cysteine proteinase releases biologically active fragments of *Streptococcal* surface proteins. *J Biol Chem*. 1995;270:9862-9867.
75. Herwald H, Cramer H, Mörgelin M, et al. M protein, a classical bacterial virulence determinant, forms complexes with fibrinogen that induce vascular leakage. *Cell*. 2004;116:367-379.
76. Schragar HM, Rheinwald JG, Wessels MR. Hyaluronic acid capsule and the role of *Streptococcal* entry into keratinocytes in invasive skin infection. *J Clin Invest*. 1996;98:1954-1958.
77. Schragar HM, Alberti S, Cywes C, Dougherty GJ, Wessels MR. Hyaluronic acid capsule modulates M protein-mediated adherence and acts as a ligand for attachment of group A *Streptococcus* to CD44 on human keratinocytes. *J Clin Invest*. 1998;101:1708-1716.
78. Penc SF, Pomahac B, Winkler T, et al. Dermatan sulfate released after injury is a potent promoter of fibroblast growth factor-2 function. *J Biol Chem*. 1998;273:28116-28121.
79. Smith MM, Melrose J. Proteoglycans in normal and healing skin. *Adv Wound Care (New Rochelle)*. 2015;4:152-173.
80. Juhlin L. Hyaluronan in skin. *J Intern Med*. 1997;242:61-66.
81. Schmid-Wendtner MH, Korting HC. The pH of the skin surface and its impact on the barrier function. *Skin Pharmacol Physiol*. 2006;19:296-302.
82. Noborn F, Gomez Toledo A, Sihlbom C, et al. Identification of chondroitin sulfate linkage region glycopeptides reveals pro-hormones as a novel class of proteoglycans. *Mol Cell Proteomics*. 2015;14:41-49.
83. Schneider LA, Korber A, Grabbe S, Dissemmond J. Influence of pH on wound-healing: a new perspective for wound-therapy? *Arch Dermatol Res*. 2007;298:413-420.
84. Shukla VK, Shukla D, Tiwary SK, Agrawal S, Rastogi A. Evaluation of pH measurement as a method of wound assessment. *J Wound Care*. 2007;16:291-294.
85. Mende M, Bednarek C, Wawrzyszyn M, et al. Chemical synthesis of glycosaminoglycans. *Chem Rev*. 2016;116:8193-8255.
86. Ayinuola YA, Tjia-Fleck S, Readnour BM, et al. Relationships between plasminogen-binding M-protein and surface enzyme for human plasminogen acquisition and activation in *Streptococcus pyogenes*. *Front Microbiol*. 2022;13:905670.
87. Raman R, Sasisekharan V, Sasisekharan R. Structural insights into biological roles of protein-glycosaminoglycan interactions. *Chem Biol*. 2005;12:267-277.
88. Sodhi H, Panitch A. Glycosaminoglycans in tissue engineering: a review. *Biomolecules*. 2020;11:29.
89. Taweechat P, Pandey RB, Sompornpisut P. Conformation, flexibility and hydration of hyaluronic acid by molecular dynamics simulations. *Carbohydr Res*. 2020;493:108026.

90. Wessels MR, Bronze MS. Critical role of the group A *Streptococcal* capsule in pharyngeal colonization and infection in mice. *Proc Natl Acad Sci USA*. 1994;91:12238-12242.
91. Cywes C, Stamenkovic I, Wessels MR. CD44 as a receptor for colonization of the pharynx by group A *Streptococcus*. *J Clin Invest*. 2000;106:995-1002.
92. Flores AR, Jewell BE, Olsen RJ, et al. Asymptomatic carriage of group A *Streptococcus* is associated with elimination of capsule production. *Infect Immun*. 2014;82:3958-3967.
93. Wessels MR, Moses AE, Goldberg JB, DiCesare TJ. Hyaluronic acid capsule is a virulence factor for mucoid group A *Streptococci*. *Proc Natl Acad Sci USA*. 1991;88:8317-8321.
94. Dale JB, Washburn RG, Marques MB, Wessels MR. Hyaluronate capsule and surface M protein in resistance to opsonization of group A *Streptococci*. *Infect Immun*. 1996;64:1495-1501.
95. Dinkla K, Sastalla I, Godehardt AW, et al. Upregulation of capsule enables *Streptococcus pyogenes* to evade immune recognition by antigen-specific antibodies directed to the G-related alpha2-macroglobulin-binding protein GRAB located on the bacterial surface. *Microbes Infect*. 2007;9:922-931.
96. Moses AE, Wessels MR, Zalcman K, et al. Relative contributions of hyaluronic acid capsule and M protein to virulence in a mucoid strain of the group A *Streptococcus*. *Infect Immun*. 1997;65:64-71.
97. Wilde S, Dash A, Johnson A, Mackey K, Okumura CYM, LaRock CN. Detoxification of reactive oxygen species by the hyaluronic acid capsule of group A *Streptococcus*. *Infect Immun*. 2023;91:e0025823.
98. Matysik A, Kline KA. *Streptococcus pyogenes* capsule promotes microcolony-independent biofilm formation. *J Bacteriol*. 2019;201:e00052-19.
99. Cedervall T, Akesson P, Stenberg L, Herrmann A, Akerström B. Allosteric and temperature effects on the plasma protein binding by *Streptococcal* M protein family members. *Scand J Immunol*. 1995;42:433-441.
100. Mills JO, Ghosh P. Nonimmune antibody interactions of group A *Streptococcus* M and M-like proteins. *PLoS Pathog*. 2021;17:e1009248.
101. Brouwer S, Barnett TC, Rivera-Hernandez T, Rohde M, Walker MJ. *Streptococcus pyogenes* adhesion and colonization. *FEBS Lett*. 2016;590:3739-3757.
102. Anderson EL, Cole JN, Olson J, Ryba B, Ghosh P, Nizet V. The fibrinogen-binding M1 protein reduces pharyngeal cell adherence and colonization phenotypes of M1T1 group A *Streptococcus*. *J Biol Chem*. 2014;289:3539-3546.
103. Molinari G, Chhatwal GS. Invasion and survival of *Streptococcus pyogenes* in eukaryotic cells correlates with the source of the clinical isolates. *J Infect Dis*. 1998;177:1600-1607.
104. Bachert BA, Choi SJ, LaSala PR, et al. Unique footprint in the scl1.3 locus affects adhesion and biofilm formation of the invasive M3-type group A *Streptococcus*. *Front Cell Infect Microbiol*. 2016;6:90.
105. Elliott SD. A proteolytic enzyme produced by group A *Streptococci* with special reference to its effect on the type-specific M antigen. *J Exp Med*. 1945;81:573-592.
106. Pählman LI, Olin AI, Darenberg J, et al. Soluble M1 protein of *Streptococcus pyogenes* triggers potent T cell activation. *Cell Microbiol*. 2008;10:404-414.
107. Davies MR, McIntyre L, Mutreja A, et al. Atlas of group A *Streptococcal* vaccine candidates compiled using large-scale comparative genomics. *Nat Genet*. 2019;51:1035-1043.
108. Walker MJ, Hollands A, Sanderson-Smith ML, et al. DNase Sda1 provides selection pressure for a switch to invasive group A *Streptococcal* infection. *Nat Med*. 2007;13:981-985.
109. Ly AT, Noto JP, Walwyn OL, et al. Differences in SpeB protease activity among group A streptococci associated with superficial, invasive, and autoimmune disease. *PLoS One*. 2017;12:e0177784.
110. Olsen RJ, Raghuram A, Cantu C, et al. The majority of 9,729 group A *Streptococcus* strains causing disease secrete SpeB cysteine protease: pathogenesis implications. *Infect Immun*. 2015;83:4750-4758.
111. Loh JMS, Tsai JC, Proft T. The ability of group A *Streptococcus* to adhere to immortalized human skin versus throat cell lines does not reflect their predicted tissue tropism. *Clin Microbiol Infect*. 2017;23:677.e1-677.e3.
112. Bucior I, Scheuring S, Engel A, Burger MM. Carbohydrate-carbohydrate interaction provides adhesion force and specificity for cellular recognition. *J Cell Biol*. 2004;165:529-537.
113. Haseley SR, Vermeer HJ, Kamerling JP, Vliegthart JF. Carbohydrate self-recognition mediates marine sponge cellular adhesion. *Proc Natl Acad Sci USA*. 2001;98:9419-9424.
114. Handa K, Takatani-Nakase T, Larue L, Stemmler MP, Kemler R, Hakomori SI. Le(x) glycan mediates homotypic adhesion of embryonal cells independently from E-cadherin: a preliminary note. *Biochem Biophys Res Commun*. 2007;358:247-252.
115. Popescu O, Checui I, Gherghel P, Simon Z, Misevic GN. Quantitative and qualitative approach of glycan-glycan interactions in marine sponges. *Biochimie*. 2003;85:181-188.
116. Bartelt MA, Duncan JL. Adherence of group A *Streptococci* to human epithelial cells. *Infect Immun*. 1978;20:200-208.
117. Grabovskaya KB, Totoljan AA, Rýc M, Havlíček J, Burova LA, Bícová R. Adherence of group A *Streptococci* to epithelial cells in tissue culture. *Zentralbl Bakteriell A*. 1980;247:303-314.
118. Courtney HS, Ofek I, Hasty DL. M protein mediated adhesion of M type 24 *Streptococcus pyogenes* stimulates release of interleukin-6 by HEp-2 tissue culture cells. *FEMS Microbiol Lett*. 1997;151:65-70.
119. Levin JC, Wessels MR. Identification of csrR/csrS, a genetic locus that regulates hyaluronic acid capsule synthesis in group A *Streptococcus*. *Mol Microbiol*. 1998;30:209-219.

SUPPORTING INFORMATION

Additional supporting information can be found online in the Supporting Information section at the end of this article.

How to cite this article: McEwan TB-D, De Oliveira DMP, Stares EK, et al. M proteins of group A *Streptococcus* bind hyaluronic acid via arginine-arginine/serine-arginine motifs. *The FASEB Journal*. 2024;38:e70123. doi:[10.1096/fj.202401301R](https://doi.org/10.1096/fj.202401301R)